N3Cat
Nanonetworking Center
in Catalunya

UPC

Diffusion-based Physical Channel Identification for Molecular Nanonetworks

Nora Garralda Torres

Master Thesis / 2010

Master of Science in Information and Communication Technologies

Master Thesis Advisors:

Albert Cabellos

Ignacio Llatser

Department of Computer Architecture

Universitat Politecnica de Catalunya, Barcelona

Abstract

Nanotechnology is the engineering of functional systems at the molecular/atomic level. Nanomachines are expected to be very simple devices, but nanonetworks, the association of nanomachines, are expected to increase their capabilities, allowing them to share information in order to perform more complex tasks and increase their range of operation. How nanomachines will communicate is currently under research. This growing research field has attracted the interest of researchers from several domains, from information and communication technologies, to nanotechnology or biotechnology and several communication alternatives have been recently proposed.

Molecular communication (MC), based on the exchange of information by releasing/absorbing molecules, is a novel communication paradigm to interconnect nanomachines that seems well-suited to the nano-scale, specially, when intra-body scenarios for medical applications are envisaged. MC spans different bio-inspired distance-based techniques for the transportation of molecules. Amongst these, diffusion-based MC, proposed for covering short distances ($nm - \mu m$), is one of the techniques that has attracted the most attention.

In this work, the diffusion-based MC channel is explored in order to extract its main communication metrics, such as attenuation and delay with respect to frequency and distance. The LTI property is proven to be a valid assumption for normal diffusion-based single/multi-transmitter scenarios. Different pulse-based modulation techniques are compared by means of throughput, operation range, energy requirements and ISI, and the optimal pulse shape for these modulations is provided. Finally, interferences are evaluated in a broadcast communication scenario and diffusion-based noise is observed and assessed with reference to already proposed stochastic models.

The exploration of the physical diffusion-based communication channel is based on simulations. *N3Sim*, a simulation framework for the general case of diffusion communication, is presented and used for the simulations.

We aim to contribute with this simulator and this study to continue the development of an appropriate channel model tailored to the physical layer singularities of

MC. As well as, to provide guidelines on molecular signaling and on communication performance of different modulation techniques for MC.

.

Acknowledgments

This work is the fruit of many people's labor, many of whom I will thank in the following lines: First of all, I would like to thank Josep Solè Pareta twice for his guidance through all this time as coordinator of my Master studies, and for introducing me to the nano group. Secondly, I'd like to sincerely thank my advisors, Albert Cabellos and Ignasi Llatser, for their advice, insight and orientation, and for their immense enthusiasm about the topic. Third, I cannot forget to express my gratitude to E.Alarcòn for his always welcome technical remarks and explanation. And last but not least, I want to thank Iñaki very much because without him this work could not have been possible, and because I deeply appreciate his help and support from the beginning. Working surrounded by all of you started as a challenge but in time has rewarded me with new experiences and knowledge, and has taught me what 'research' is about.

I am also very grateful to the Nanonetworking Center in Catalunya, and to Prof. Akyildiz for giving me the opportunity to go to Atlanta. Words cannot express my gratitude to all the BWN lab team because they made me feel at home from the day I arrived. Special thanks go to Massimiliano Pierobon for his tireless patience and sharing of knowledge.

To finalize, I am going to take this opportunity to express my gratitude to my family for their support, and love that always helps me, to my friends, specially to the ones I have met during the course in this university, for the confidence I received from them, and to Pablo for showing always admiration for this work and for making me easier to go on in my every day work.

Contents

1 Introduction **1**

1.1 Motivation 1

1.2 Goals and expected results 3

1.3 Structure of the thesis 5

2 State of the art **7**

2.1 Molecular Communication 7

2.1.1 Introduction 7

2.1.2 Classification 9

2.2 Biosignaling 11

2.2.1 Introduction 11

2.2.2 Reception: Ligand-binding Theory 12

2.3 Kinetic Theory 13

2.3.1 Diffusion 13

2.3.1.1 Microscopic view of Diffusion 13

2.3.1.2 Macroscopic view of Diffusion 15

2.3.2 Anomalous Diffusion 17

2.3.2.1 Microscopic view of Anomalous Diffusion 17

2.3.2.2 Macroscopic view of Anomalous Diffusion 18

2.3.2.3 Electrodiffusion 19

3 Diffusion-based Simulators **21**

3.1 Related work 21

3.2 N3Sim Introduction 22

4 Channel Identification 27

4.1 Introduction 27

4.1.1 Channel Linearity and Time invariance 28

4.2 Channel Identification Methods 32

4.2.1 Excitation Signals Overview 32

4.2.2 Impulse excitation analysis 33

4.2.3 PRBS excitation analysis 35

4.3 Channel Identification Results 38

4.3.1 Normal Diffusion-based Channel 38

4.3.2 Anomalous Diffusion based channel 41

4.4 Dispersive channels 44

4.5 Molecular Signaling 46

4.5.1 Path loss curve 47

4.5.2 Environmental sensibility 48

5 Modulation Schemes Comparison 51

5.1 Introduction 51

5.2 Pulse-based Modulation Techniques 52

5.2.1 Pulse shaping 52

5.2.2 Analytical Comparison 56

5.2.3 Simulation-based Comparison 59

6 Noise Analysis and Interference Evaluation 65

6.1 Noise Analysis 65

6.1.1 Noise sources Overview 65

6.1.2 Noise models validation results 67

6.2 Interferences Evaluation 68

7 Conclusions and future work 73

7.1 Conclusions 73

7.2 Future Work 76

Bibliography **76**

Chapter 1

Introduction

This chapter states the motivation and goals of this thesis and presents its overall structure.

1.1 Motivation

Nanonetworking is an emerging field of research, where nanotechnology and communication engineering meet on a common ground. Nanotechnology is the science of manipulating matter on the atomic and molecular scale, which ranges from one to a few hundred nanometers. The first concepts in nanotechnology were identified by Richard Feynman in 1959, in his talk "There is plenty of room at the bottom". He introduced the idea of manipulating and controlling things on a small scale; *i.e.*, fabricating wires with dimensions ranging from 10 to 100 atoms, while in that time, computers were filling rooms.

Nanotechnology is intuitively envisaged as the miniaturization of the existing microtechnology. This fabrication technique encounters problems due to physical limitations when decreasing the size of existing silicon-based solutions. Moore's law can no longer be applied when following this top-down approach of fabrication, because quantum effects appear in the nanoscale changing the rules governing traditional electromagnetic (EM) technology [3]. However, a generation of new materials has been proposed in order to avoid some of these problems, and it has opened the door

to a bottom-up approach of fabrication.

A nanomachine is the most basic functional unit that works at the nano-scale, able to perform simple tasks such as computing, sensing, data storing, or actuation.

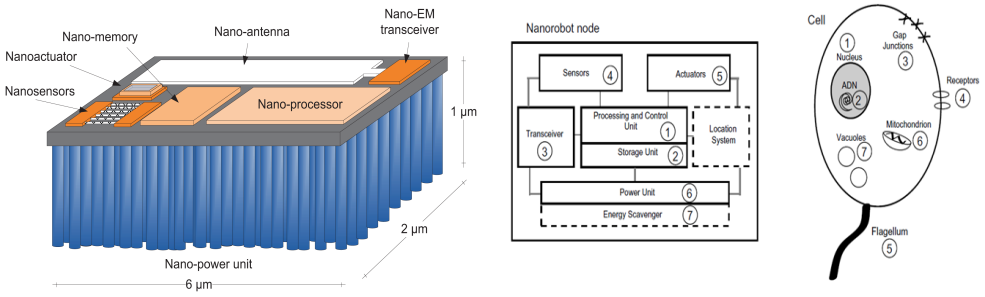

Figure 1.1: a) Conceptual scheme of an EM-nansensor [3]; b) Conceptual scheme of a biological nanorobot [2].

Nowadays nanotechnology covers two main lines of research. On the one hand, research into graphene-based nanomachines. Carbon Nanotubes, and Graphene Nanoribbons have been the recently proposed carbon materials that present extremely conductive properties and are about 20 to 40 times smaller in diameter than nanowires [30]. On the other hand, research into biological or hybrid nanomachines. The bio-nanodevices will be fabricated by manipulating existing molecular components and/or joining them to artificial counterparts. A recent study [1] shows that in 1 gram of bacteria 90GB can be stored.

Fig.1.1.a shows a conceptual scheme of an EM-nanosensor and fig.1.1.b shows a conceptual scheme of a biological-nanorobot.

While isolated nanomachines are expected to perform very simple tasks, nanonetworks, the interconnection of nanomachines, are expected to expand their capabilities, allowing cooperation among nanodevices in order to perform more complex tasks and increase their operation range [2]. There are two novel communication paradigms in the nano-scale that will allow the implementation of nanonetworks:

1. **Graphene-based EM Communication**, based on the exchange of information by sending/receiving electromagnetic waves [24]. (E.g., Wireless NanoSensor Networks [3], [9]).

2. **Molecular Communication**, MC, a novel bio-inspired communication paradigm where information is shared by the exchange of molecules.

Nanonetworks are expected to be applied in many different fields: from the environmental to the industrial and to the biomedical. These possible applications include:

- Drug delivery systems, or diagnostic and therapeutic antiviral activities are two examples within the biomedical field. More specific applications in medicine and biology are enumerated in [43] and [15].
- Catalysis, filtration and energy storage within the environmental field.
- Semiconductor devices, memory storage, and quantum computers amongst others, in the ICT field. Furthermore, in recent years, there have been attempts to create bio-computers, in which nano-scale logic gates and memory chips are fabricated by means of bio-components [44], [30].

Potential applications are expected from molecular nanonetworks. Nanonetworking is still a novel research field, therefore, how nanomachines will communicate is an open issue. This master thesis focuses on exploring a communication channel already proposed in the literature to cover short operation distances based on the diffusion of molecules. The next chapter (Section 2.1.2) introduces an overview about the proposed communication techniques that form molecular communication.

1.2 Goals and expected results

This Master Thesis focuses on identifying the diffusion-based communication channel for molecular nanonetworks in order to extract its main communication metrics. Molecular signaling is a bio-inspired communication technique where the information is encoded in the concentration of molecules in the environment. A transmitter nanomachine suspended in a fluid medium emits molecules changing its local concentration, according to a release pattern which encodes the transmitted information.

A net flux of particles appears upon the concentration gradient and propagates towards the homogenization of the concentration. The propagation of the molecules is known as diffusion and it is mathematically modeled by Fick's laws. The created changes in concentration eventually reach the receiver nanomachine located at a certain distance. The receiver nanomachine measures the concentration and decodes the transmitted information by following the ligand-binding theory.
In the literature there are several analytical studies approaching the channel modeling for the molecular signaling alternative, as well as approaching the capacity from an information theory perspective. Section 2.1.2 mentions the most relevant studies regarding this topic. In order to validate the existing models and provide a common ground to compare them, tests either by means of simulation or experimentation should also be provided. Due to the lack of simulation tools and the high costs of performing real experiments in order to validate the analytical channel models for diffusion-based MC, we decided to implement *N3Sim*, a simulation framework for the general case of diffusion-based communication. Its main characteristics are introduced in Section 3.2.
From this chapter on, we will explore the following questions and open issues:

- How do interactions among the diffusing molecules change the diffusion process? When is it valid to use Fick's Laws of diffusion to model the diffusion process, and when are other alternatives needed? These questions are explored in Section 2.3 in an theoretical way, where different diffusion scenarios are explained. Moreover, this topic is approached by means of comparison of simulation results in Section 4.3.

- Is the diffusion-based communication channel linear and temporal invariant for the single-transmitter scenario? What is the channel transfer function of this channel? (Addressed in Sections 4.1.1 and 4.3).

- Is the diffusion-based communication channel linear and time invariant for the multi-transmitter scenario when transmitting the same type of molecules? Are there differences if transmitting different types of molecules?. (Addressed in

Sections 4.1.1, 4.3 and 6.2) .

- What are the transmission power requirements to cover a given range? (Analyzed in Section 4.5.1)
- How sensible is this communication scenario to environmental changes such as temperature/ fluid viscosity / carrier size variations? The communication scenario contains a fluid and usually a certain homogeneous concentration of particles of the same type as information particles. How does this concentration affect the transmission and reception of information? (Discussed in Section 4.5.2).
- How can information be more efficiently transmitted using different modulation techniques? A discussion about possible modulations techniques as well as the obtained results of simulation comparison are found in Section 5.2.
- How much uncertainty is added by the random motion of the particles? Are there more noise sources? (Addressed in Section 6.1.2, where noise sources are compared and evaluated with already proposed stochastic models from [39]).
- In a broadcast communication scenario, how do interferences affect the reception process? (Addressed in Section 6.2)

Exploring the physical layer is the first step to develop appropriate architectures and protocols for higher layers of the molecular communication stack.

1.3 Structure of the thesis

This thesis is organized as follows. Chapter one states the motivation and goals of the thesis. Chapter two outlines the state-of-the-art of each of the different fields that are involved in the development of this research. Chapter three gives an overview of *N3Sim*. Chapter four explains the methodology and the obtained results for the identification of the diffusion-based communication channel. The fifth chapter analyzes and compares different modulation schemes in order to find the one that

suits best in this communication alternative. Chapter six analyses the noise sources and interferences among transmitters in a broadcast scenario. Finally, chapter seven develops the conclusions and contributions of this thesis, and identifies open issues and necessary future work.

Chapter 2

State of the art

This chapter outlines the state-of-the-art of the molecular communication paradigm. In addition, it introduces the kinetic theory and some key biological concepts.

2.1 Molecular Communication

2.1.1 Introduction

Molecular communication allows the implementation of molecular nanonetworks. The first concept on molecular communication to implement nanonetworks were identified in [44]. Nanodevices, bio-inspired, hybrid or manufactured, within a molecular nanonetwork will own bio-transceivers that will be able to react to specific molecules, and to release others in response to an internal command.
Molecular nanonetworks are especially aimed to intra-body scenarios due to their low power requirements and their high bio-compatibility. An example of an intra-body nanonetwork with health-care monitoring perspectives is shown in Fig. 2.1.
Two different and complementary encoding techniques can be used for the general case of molecular communication.

1. *Concentration Encoding.* It consists in encoding the information changing the temporal transmission of particles. (E.g. changing the concentration level in the space.)

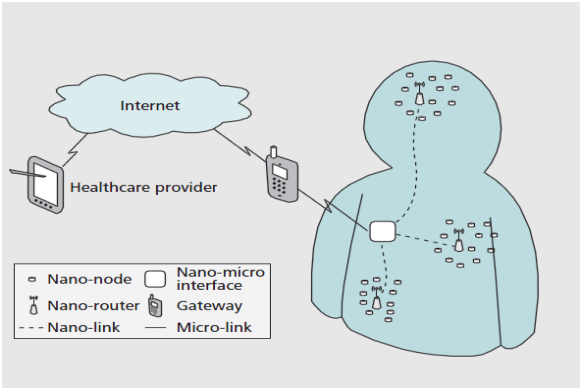

Figure 2.1: Intra-body nanonetworks for health-care applications [4].

Communication	**EM/optical**	**Molecular**
Carriers	Electrical/Optical signals	Chemical signals
Environment	Wires/airbone	aqueous/fluids
Velocity	High speed	Slow velocity
Range	[m-Km]	[nm-m]
Energy consumption	High requirements	Energy efficient
Transmission accuracy	High accuracy	Low accuracy, Stochastic effects

Table 2.1: Traditional Communication Vs Molecular Communication

2. *Molecular Encoding.* It consists in encoding the information into internal parameters of the sent molecules (E.g. changing the molecule type).

Table 2.1 shows the main characteristics of MC, by comparison to traditional communication techniques. MC shows distinctive features that are not found in the current method of telecommunication based on electrical or optical signals. MC allows very slow signal transmission over a limited range, but communication by the exchange of molecules is possibly deployable directly on the nano-scale presenting very low power requirements.

Molecular communication differs from the conventional communication paradigms (such us acoustic, EM, ...), hence, appropriate information theory and communications models are required.

2.1.2 Classification

Molecular communication includes several communication solutions depending on how molecules propagate in the medium:

- In *Diffusion-based* molecular channel, particles are immersed in a fluid medium and they spontaneously spread in the space upon a concentration gradient tending towards the homogenization of the concentration in the fluid, hence increasing the entropy of the fluid.

  In biology, diffusion occurs in several scenarios, for example: 1) within a cell: calcium signaling in intra-cell communication, 2) between cells: calcium signaling through gap junctions, 3) among organisms: transportation of pheromones in ant colonies.

  Different bio-inspired scenarios of diffusion-based channels have been proposed in the literature. Among others, in [31] an introduction for the modeling of a communication channel based on calcium signaling inspired by intra-cellular communication is proposed, and in [34] a communication channel inspired by inter-cellular communication where the transmitted signals propagates by means of diffusion through extra-junctional connexions is presented. Furthermore, the usage of pheromones for a long range diffusion-based communication channel is proposed in [5].

  Several authors have addressed the channel modeling for diffusion-based communication solutions following mathematical approaches. Amongst others, [40] describes one scenario of diffusion-based communication channel and depicts the final attenuation and delay for different distances and frequencies. In [29], an energy model is presented for communication via diffusion.

  Furthermore, in the literature there are different research efforts addressing the information capacity of the diffusion-based molecular channel in an analytical way, such as [8], [7], [25],[6], [41].

  Fig.2.2 represents a conceptual scheme of how information is transmitted over a diffusion-based communication channel for molecular nanonetworks.

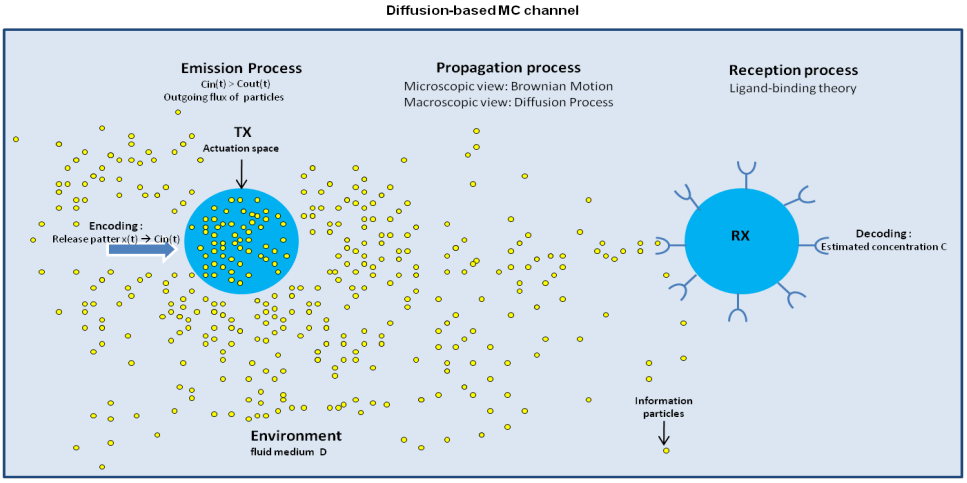

Figure 2.2: Diffusion-based molecular communication channel conceptual scheme.

- In a *Flow-based* molecular channel, particles are immersed in a constrained fluid medium. The fluid contains a drift velocity which is on top of the diffusion process, *i.e.,* hormones in the blood and pheromones in windy air in ant colonies.

  The capacity of this channel is approach in [26] from an information theory perspective.

- In a *Walkway-based* molecular channel, the transport of the information is active and mediated by intermediary molecules, e.g. molecular motors or flagellated bacteria. In the first case, the dynein molecular motor carries proteins by sliding over the microtubules in cells, and in the second case, a bacterium swims towards chemicals attractants released by the receiver using flagella. In both cases, *Molecular encoding* is applied, the transmission of information is based on encoding the information in DNA sequences and using molecular motors or flagellated bacteria as transportation mechanisms.

  A communication using molecular motors was proposed in [33] and a study about using bacteria is presented in [17] .

In a *diffusion-based* communication channel the transport time relies on the concentration gradient, it is usually a very slow process that does not require energy, however, the active transport found in the *walkway-based* channel, requires energy

in order to transport the information.

The range of operation depends on the communication alternative. For short distances (nm-μm) molecular motors or calcium signaling are recommended [2], for medium range (μm-mm) the usage of the flagellated bacteria [19] or catalyctic nanomotos [18] are suggested, and for long range (mm-m) communications by pheromones have been proposed [5].

2.2 Biosignaling

2.2.1 Introduction

Biosignaling is the ability to receive signals and act upon the information extracted from those signals. Cell receptors convert the information into a cellular response which involves a chemical process. Each signal elicits appropriate responses such as motion toward food in bacteria, or metabolic activities in animal cells. This process is used by any living organism from bacterial cells to hormones. The conversion of information into a chemical change is known as signal transduction [35].

Calcium signaling has been proposed as a communication technique to cover short distances. Calcium ions (Ca^{2+}) constitute one of the most important intracellular second messengers, covering a wide range of actions. Diffusion is the means whereby calcium ions move from a position to another one. Changes in Ca^{2+} concentration trigger intracellular responses such as exocytosis or contraction in muscles. The concentration of Ca^{2+} is normally kept constant and very low, and when an activating signal arrives, calcium concentration increases, triggering the receptors, thus, producing the intracellular process. When the process has ended, the Ca^{2+} concentration decreases again. For example, the normal Ca^{2+} concentration in the intra-cellular fluid is lower than 10^{-7} Molar. When a process such as the muscle contraction takes place in few seconds the Ca^{2+} concentration increases reaching levels of 10^{-4} Molar [21].

2.2.2 Reception: Ligand-binding Theory

The reception process (receiving and recovering the information) for the molecular signaling communication technique is based on the Ligand-binding theory.
A molecular receiver has a number of receptors on its surface. This theory is based in two possible reaction kinetics:

1. A successful reaction: the ligand molecules A, when encountering receptors R, constitute the bound receptors, producing complexes C, generating a concentration in the receiver side, thus allowing the receiver to understand the biological information:

$$A + R \overset{K_1}{\rightarrow} C \tag{2.1}$$

   where K_1 is the binding rate, which indicates the ratio of molecules binding to the receptors.

2. An unsuccessful reaction: the ligand molecules A, when encountering receptors R, are released, not forming complexes C, not becoming bounded molecules, thus, not allowing the receiver to understand the information:

$$A + R \overset{K_{-}1}{\leftarrow} C \tag{2.2}$$

   whereK_{-1} is the releasing rate which indicates the ratio of the molecules being released from the receptors.

The binding rate depends on diffusion parameters, such as the diffusion coefficient, the temperature, and the distance between the transmitter and receiver. In the releasing rate more factors are involved and it follows a non-linear relation to the diffusion parameters.

2.3 Kinetic Theory

2.3.1 Diffusion

Kinetic Theory is the molecular theory of gases which states that matter is made up of smaller particles, atoms or molecules, which are always moving randomly, in order to explain the macroscopic properties that gases show.

2.3.1.1 Microscopic view of Diffusion

Many identical particles under the same boundary and initial conditions share statistical properties of their spatial and temporal evolution exhibiting the diffusion process. The diffusion equation describes the macroscopic view of these movements, defining how we (in our scale) perceive it, but the individual movement of each particle is not governed by the diffusion equation.

Life of small particles is dominated by fast time scales, short distances and collisions with neighboring particles that yield a very erratic motion. The bridge between the microscopic and the macroscopic world was built by A. Einstein [37].

Brownian Motion, BM, is the random process that underlies diffusion. BM is the never-ending movement of particles in suspension in a fluid due to all the collisions the suspended particle suffers with the particles from the fluid in all directions.

While BM was first explained by Brown, Einstein derived its mathematical form, showing at the same time that matter was made up of small particles.

Einstein first expressed the diffusion coefficient or Stokes-Einstein relation (S-E), with the following formula:

$$D = \frac{KT}{\pi 6Rv} \tag{2.3}$$

where K is the Boltzman constant, T is the temperature, R is the suspended particle radius and v is the fluid viscosity.

The diffusion constant is defined for diffusion of spherical particles through liquid with low Reynolds number.The Reynolds number, R_e, is a dimensionless number that expresses a ratio between inertial forces and viscous forces for a given flow condition. Inertia is the property of an object to remain at a constant velocity,

unless an outside force acts on it.Viscosity is the resistance of a fluid to flow under the influence of an applied external force. It is defined as:

$$R_e = \frac{\rho v_s r}{v} \tag{2.4}$$

where v_s is the characteristic speed the particle experiments in that fluid, r is the particle radius and ρ and v are the density, and the viscosity of the medium respectively. Being in low Reynolds number conditions means that viscous forces dominate the particle motion.

The theory of Brownian Motion was developed to describe the dynamic behavior of particles whose mass and size are much larger than those of the host medium particles [14]. In consequence, the ratio between the solute and the solvent molecules size is an important parameter. In [10] there is an explanation for anomalous diffusion which takes place when the following expression is not satisfied:

$$\frac{Rs}{Rf} > 6 \tag{2.5}$$

where R_s is the solute particle radius and the R_f is the solvent particle radius.

When the previous equation is not satisfied some modifications are proposed to the computation of the diffusion coefficient. Usually when this ratio decreases, diffusion is enhanced.

An approach of how to change the diffusion coefficient when the sizes of solvent and solute are comparable, is addressed in [27], where it is proposed to add a multiplicative correction term that affects to the diffusion coefficient computation ($D' = D\alpha$), according to the ratio among particle sizes:

$$\alpha = 1 + (\frac{R_f}{R_s})^{1/3} \tag{2.6}$$

In [29], there is another approach addressing the same problem, where they propose to modify the diffusion coefficient by adding a multiplicative factor α equal to $\frac{3}{2}$ when the propagating molecule's size is very close to the size of the particles from

the fluid.

Secondly, Einstein, mathematically described the BM by defining the root mean square displacement particles suffer in each axis during an interval t:

$$\langle x \rangle = \sqrt{2Dt} \tag{2.7}$$

The time scale has to be long compared with the typical intervals of collisions among the molecules, which are around 10^{-12} [46], to obtain valid results.

Brownian Motion is also known as Wiener process, it is a continuous time stochastic process which belongs to the Lévy processes.

2.3.1.2 Macroscopic view of Diffusion

Diffusion was first described as the irregular motion of coal dust on the surface of alcohol by Jan Ingenhousz and as a the jittery motion of pollen grains in a fluid by T. Graham [47]. After that, Fick, analytically modeled the diffusion process with the development of Fick's laws of diffusion. He did the analogy between diffusion and conduction of heat or electricity, assuming that the flux of matter is proportional to its concentration gradient with a substance-dependent proportionality factor.

First Fick's Law gives an expression to quantify the net flux of particles that appear upon a concentration gradient, as the number of particles that moves through a unit measure and unit time:

$$J = -D\nabla C \tag{2.8}$$

where D is the diffusion coefficient, J is the particle flux and ∇C the concentration gradient vector with the same dimensions as the space.

The Continuity principle concept states that matter cannot be created or destroyed, declaring that changes in concentration in the space are only possible if there is an inflow or an outflow flux of concentration into or out to the system. This is mathematically captured by the following expression:

$$\frac{dC}{dt} + \nabla J = 0 \tag{2.9}$$

The second Fick's Law also known as the Fundamental law of Diffusion, is derived straightforward from this principle by substituting the derivative of the flux from Eq.2.8 into Eq.2.9. This law describes the concentration field, *i.e.*, how concentration in space changes over time.

$$\frac{dC}{dt} = D\nabla^2 C \tag{2.10}$$

where ∇^2 is the Laplace operator.

The Green function of the Diffusion equation is the answer to the Delta input, and has the following expression:

$$\begin{aligned} G(\bar{x}, \bar{x}', t) &= \frac{1}{(2\pi)^{n_{dim}}} \int_s e^{-D\|\bar{k}\|^2 t} e^{j\bar{k}\|\bar{x}-\bar{x}'\|} \, , d\bar{k} \\ &= \frac{1}{(4\pi Dt)^{0.5 n_{dim}}} e^{-\frac{\|\bar{x}-\bar{x}'\|^{\,2}}{4Dt}} \end{aligned} \tag{2.11}$$

where n_{dim} is dimension of the space.

Fick's laws models the diffusion process of a moderate concentration of molecules, so that each molecule can be considered as independent [14], but fails for modeling the diffusion process of a high concentration of propagating molecules due to interactions among diffusion particles change the diffusion process. The latter case is known as Collective diffusion.

The lack of correlation in following Brownian steps has two important consequences, the first one is that particles move with infinite velocity, and the other is that the motion of the dispersing particles is not predictable even on the smallest time scales, characteristics that are not realistic and lead the diffusion not to satisfy the Relativistic principle [32]. This is reflected in the diffusion equation solution which allows some probability, though exponentially small, that a dispersing particle will travel arbitrarily far from its current position in any small but nonzero amount of time, thus, exceeding the speed of line. Despite this feature, the equation satisfactorily describes diffusion in many different scenarios.

2.3.2 Anomalous Diffusion

The general diffusion process that can not be mathematically modelled by Fick's Laws is known as anomalous diffusion.

2.3.2.1 Microscopic view of Anomalous Diffusion

Brownian dynamics defines the mean square displacement a molecule experiences in each direction with the linear relation with time: $\langle x \rangle^2 \propto t^\alpha; \alpha = 1$
When this linearity is lost the resulting diffusion process is known as anomalous diffusion, and the previous formula is satisfied for $\alpha < 1$ or $\alpha > 1$. Those values lead to a subdiffusion process (slower) or a superdiffusion process (faster) respectively.
In biology superdiffusion is usually found when: 1) there are interactions among the colloids that add external forces to the normal diffusion accelerating the spread process, such as charge repulsion among the particles as in the case of ions, or 2) when the fluid medium owns a drift velocity, as it happens in the blood. Subdiffusion is usually found when there are obstacles in the medium, such as the organelles present in the cytolitic liquid within a cell.
The mathematical process underlying anomalous diffusion is the correlated random walk, CRW, from the family of Random walks also belonging to the Lèvy processes. Random walks, are a family of process where molecules always experience the same step size, $\triangle x$, during constant intervals, $\triangle t$, which leads to find particles traveling at a constant speed, $\gamma = \dfrac{\triangle x}{\triangle t}$, while the uncertainty resides in the direction of each step.
CRW is a discrete process which includes memory [47], this contrasts with BM, whose main feature is the absence of time correlation, thus being a memoryless process. Particles changes its previous direction with a certain probability $\beta = \mu \triangle t$, or remain in the same one following the probability $1 - \beta$, where μ is the frequency of turning.
Correlated random walk spans all types of random walks [32]. The balistic motion corresponds to the extreme case of $\mu \to 0$ and diffusion motion when $\mu \to \infty$.

2.3.2.2 Macroscopic view of Anomalous Diffusion

The macroscopic view of CRW is modeled by the hyperbolic diffusion equation (or Telegraph equation), which corresponds to a modification of the Diffusion equation by the addition of a relaxation time:

$$\tau \frac{d^2C}{dt^2} + \frac{dC}{dt} = D\frac{d^2C}{dx^2} \tag{2.12}$$

where τ is the correlation time which is defined as $\tau = \frac{1}{2\mu}$ and the diffusion coefficient D corresponds to $D = \frac{\gamma^2}{2\mu}$ being μ the frequency of turning and γ the particle's speed.

This equation converges to the Diffusion equation when $\tau \to 0$.

The solution to this equation is defined [32] as follows:

$$G(\bar{x}, \bar{x}', t) = \frac{1}{\sqrt{4D\tau}} e^{-\frac{t}{2\tau}} I_0\left(\frac{1}{\sqrt{4D\tau}}\sqrt{\frac{Dt^2}{\tau} - x^2}\right); for \|\bar{x}\| < \sqrt{\frac{D}{\tau}}t \\ = 0; otherwise \tag{2.13}$$

where I_0 is the modified Bessel function. It is defined 0 for other values of x. This solution unlike the Green function of Fick's laws satisfies the Relativistic Principle. Collective diffusion corresponds to the anomalous diffusion a group of particles exhibit due to the group of dispersing particles is very high and interactions among the particles add extra forces to the normal diffusion process. Depending on whether the interactions among particles are repulsive or attractive, the process scenario will be superdiffusive or subdiffusive, respectively. Interactions among the particles change the diffusion process unless the mix is ideal, which is the case when collisions among the particles from the fluid and the suspended particles, are equivalent to those among the suspended particles themselves.

Usually, collective diffusion is modeled with a space-dependent diffusion coefficient, as it is done for inhomogeneous systems. The net flux of particles can then be obtained by using the Fokker-Planck equation [11], shown next, instead of through the

first Fick's law:

$$J(x,t) = -\frac{\partial D(x)c(x,t)}{\partial(x)} \tag{2.14}$$

2.3.2.3 Electrodiffusion

Electrodiffusion is the term used for the diffusion of particles with charge, in which a deterministic drift velocity induced by an electrical field appears as part of the diffusion process. It is encountered in for instance trans-membrane transport through gated ionic channels, where the field is induced by the ionic concentration gradient across the membrane.

The diffusion coefficient is defined for this process as [23]:

$$D = \frac{\mu_q KT}{q} \tag{2.15}$$

where q is the electrical charge of a particle and μ_q the electrical mobility of a particle.

The electrical mobility is the relation between the drift velocity and the applied Electric field: $\mu_q = (-\nu/\frac{dV}{dX})$ where ν is the drift velocity (velocity a particle takes under uniform electric field conditions) and $\frac{dV}{dX}$ is the applied Electric field. [23] explains when it is valid to use BM theory for analyzing features of individual trajectories of ions: the time scale of interest has to be long compared with the velocity correlation time. The velocity correlation time is defined as:

$$\tau = \frac{mD}{KT} \tag{2.16}$$

Thus according to the ion mass, and the obtained diffusion coefficient the individual displacement of iones can be well modeled by the Brownian dynamics.

Chapter 3

Diffusion-based Simulators

This chapter gives an overview of existing diffusion-based simulators and it introduces *N3Sim*, the simulation framework we have used to fulfill this work.

3.1 Related work

There are several diffusion-based simulators in the literature, but most of them have not communication perspectives, they are mainly aimed for the study of fluid dynamics or for the research into bio-molecular processes. They implement diffusion but do not allow the obtaining of communication metrics. Therefore, are not useful for us to explore the MC channel.

Flow3D[1], a tool for the computational modeling of fluid dynamics, *Cellware*[2], a tool for modeling cellular transactions, or *Spresso*[3], a biomolecular simulator to study the particle's behavior within a fluid under the influence of a electric filed, are just some examples. There are also simpler diffusion-based simulators with educational perspectives that show graphically the diffusion of a single particle or a group of particles.

To the best of our knowledge, the existing diffusion-based simulators with communication perspectives are mentioned in the following lines:

[1] http://www.flow3d.com
[2] http://www.bii.a-star.edu.sg/achievements/applications/cellware/
[3] http://microfluidics.stanford.edu/spresso

The simulator developed by Michael Moore [4]. It models two communication techniques: diffusion-based and walkway-based. The diffusion-based technique is implemented for the diffusion of single molecules, not allowing the diffusion of a group of molecules.

In [25] the shown results for diffusion transport are validated with a diffusion simulator that only allows the diffusion of single molecules.

NanoNS [20] is a recent network simulator for the modeling of molecular nanonetworks where nodes communicate through diffusion. It is an open-source discrete event-driven network simulator made to be integrated in NS-2. The diffusion process is implemented by following the first Fick's Law, the space becomes a lattice and the net flux of particles is computed according Fick's laws. Through *NanoNS*, interactions among particles cannot be simulated. Hence, it is not useful for us either to explore the general case of diffusion-based communication.

After reviewing the existing simulators, we decided to develop a diffusion-based molecular simulator in order to be able to study the physical layer of the diffusion-based communication channel for molecular nanonetworks. I have participated in the design of the diffusion simulator, implemented by Iñaki Pascual. As mentioned in Section 2.3.2, there are scenarios when the diffusion process does not suit perfectly with Fick's Laws, so we decided to base *N3Sim* on the process that underlies diffusion. *N3Sim* models the motion of every single molecule independently, molecule by molecule, following the dynamics of Brownian Motion. Next section introduces this simulator.

3.2 N3Sim Introduction

N3Sim[5] is a simulation framework for the general case of diffusion-based molecular communication, which simulates the diffusion process by modeling each individual particle's displacement according to Brownian dynamics. *N3Sim* allows to simulate interactions among particles, such as elastic collisions and/or electrostatic interac-

[4] http://www.ics.uci.edu/~mikemo/

[5] Available at NaNoNetworking Center in Catalunya, http://www.n3cat.upc.edu/n3sim

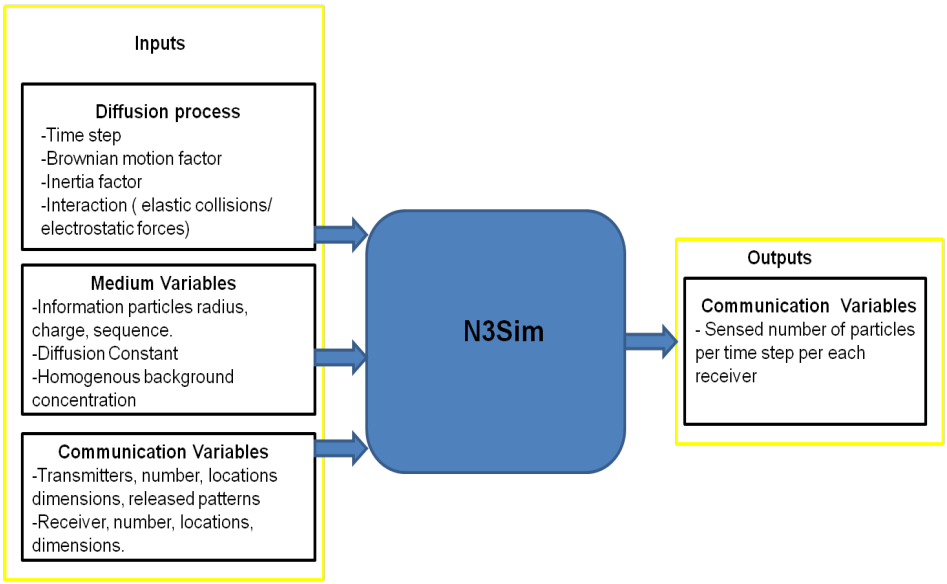

Figure 3.1: N3Sim conceptual scheme

tions, the latter case for particles that own an electrical charge. As an extension of Brownian motion, *N3Sim* simulates an estimation of a correlated random walk allowing to simulate some cases of anomalous diffusion, in which the randomness of the motion is decreased by adding inertia to the displacement of each particle.

N3Sim allows to explore the physical layer of a diffusion-based communication channel for molecular nanonetworks. Fig.3.1 shows a conceptual scheme of *N3Sim*. The outgoing files are the number of particles sensed by each receiver over time in separated files (.csv), and a video file with the whole diffusion process.

Some of the input parameters editable by the user are: the number and shape of transmitters/receivers (as well as their locations), the radius and charge of emitted molecules, the emission pattern for each transmitter, the fluid viscosity, the diffusion coefficient, and a bounded/unbounded space.

When the space is bounded, dimensions are editable. This option allows to simulate a signal transmission with a background homogeneous concentration. In this case, 2 options are available: modeling an infinite space by keeping the internal concentration in the appropriate level or modeling a bounded space where, the internal concentration grows.

Several transmitter and receivers can be simulated simultaneously. Transmitters

send the information by releasing/absorbing particles to the medium, thus changing the local particle concentration. The concentration pattern can be defined by the user or can be chosen among one of the pre-defined waveforms available in *N3Sim*, such as spikes, single pulses, or square trains, or it can be customized by the user. Through *N3Sim*, the user may choose how the transmitter encodes the information:

- Into the number of emitted molecules, known as information molecules. It can release the particles within its actuation area, or it can be defined as a punctual transmitter. For the latter case, interactions among the information particles cannot be added to the simulation.

- Into the molecule concentration at the transmitter location. The transmitter measures the concentration within its actuation area and releases/absorbs particles to/from it in order to reach a target concentration.

In both cases, an initial radial velocity can be added to the release of particles. Receivers recover the information by sensing their local concentration by counting the number of molecules within their actuation space over time. The user may also choose between two types of receivers:

- An ideal receiver transparent to the diffusion process. It counts the number of particles within its actuation area.

- A receiver that absorbs the molecules after they enter into its actuation area.

N3Sim implements the normal diffusion process for the case of two/three-dimensional space. However, when adding interactions among the particles, the space is restricted to the case of two dimensions, due to the computational cost highly increases in this case. When collisions are activated, the time complexity of the simulation algorithm increases as $O(n^3)$, being n the number of particles.
Brownian dynamics defines the motion of each particle in each direction with a Gaussian distribution independent for each dimension with zero mean and variance: $\sigma = \sqrt{2Dt}$, being D the diffusion coefficient, and t the time step. When interactions are activated, they are implemented on top of Brownian Motion. Moreover, inertia

can be added to the Brownian displacement by maintaining part of the previous velocity, to the actual one, for each particle. The parameter which controls this option is called, Inertia Factor, ranging from 0 to 1. In the latter case, the motion of the particles in no longer random.

The benefits of *N3Sim* with respect to other diffusion-based molecular communication simulators come from the fact that it simulates the motion of every single molecule independently. This allows for the observation of the effect of the molecules interactions and the uncertainty introduced by the Brownian motion. Moreover, *N3Sim* allows the simulation of scenarios having virtually any number of transmitters and receivers. This feature enables simulations where the molecular information is broadcast from one transmitter to many receivers, or where more than one transmitter access the channel at the same time.

Chapter 4

Channel Identification

This chapter explains the methodology and shows the obtained results for the diffusion-based physical channel identification.

4.1 Introduction

Channel identification is the process of modeling a channel through mathematical expressions in order to obtain a set of parameters which fully characterizes it, allowing predicting any outgoing signal for any input signal in advance, and basing the obtained expressions on measured data [42].

We consider the channel's behavior to be deterministic and we follow a non-parametric approach due to a priori knowledge of the channel is not needed, hence, we treat the channel as a black box.

We first validate the linearity and time invariance of the channel, in order to identify the channel with a linear channel model, in which, the finite impulse response (FIR) embodies all significant characteristic features of the channel. The FIR is mathematically defined for any input/output relation as:

$$y(k) = \sum_{i=1}^{n} g(i)x(k-i) + d(k) \tag{4.1}$$

where x is the input signal, y is the output signal and g the impulse response.

4.1.1 Channel Linearity and Time invariance

A LTI channel maintains its features over time as well as fulfills the superposition principle.

We check whether the diffusion-based communication channel fulfills the LTI property or not, for the diffusion process where interaction among the diffusing calcium particles (elastic collisions) are taken into account, and distinguishing among two cases: the single-transmitter scenario and the multi-transmitter scenario, both represented in Fig. 4.1:

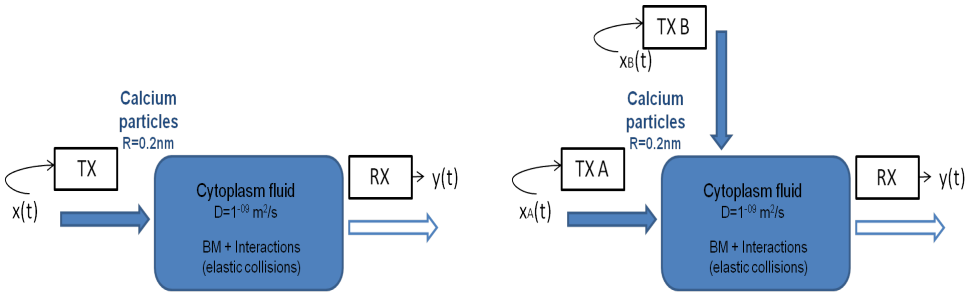

Figure 4.1: a)Single-transmitter scenario b)Multi-transmitter scenario. Calcium particles are the information particles immersed in cytoplasm fluid for both scenarios.

I) Single-transmitter scenario analysis:

In order to validate the linearity of the channel, we check if the channel satisfies the homogeneity and the addition properties by simulating three transmission/reception cases in the single-transmitter scenario (Fig.4.1.a).

First, the transmitter releases particles following a release pattern, *i.e.*, $x_1(t)$. The particles by following the Brownian dynamics as well as colliding among them eventually reach the receiver located at a certain distance, which measures the number of particles over time, $y_1(t) = f(x_1(t))$. Secondly, the transmitter releases particles following a different release pattern, *i.e.*, $x_2(t)$ and we measure the output, $y_2(t) = f(x_2(t))$. Thirdly, we use the addition of both previous transmitted signals as the new release pattern, $x_3(t) = x_1(t) + x_2(t)$, and we measure the output, $y_3(t) = f(x_3)$. Finally we check whether the output matches with the addition of

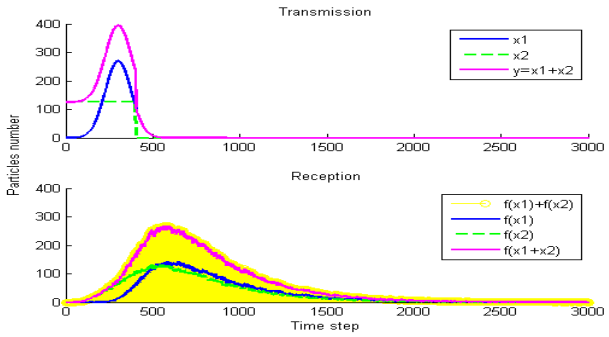

Figure 4.2: Linearity validation for the single-transmitter scenario. Transmission (upper image) and reception (lower image) of a Gaussian pulse, a square pulse and the addition of both.

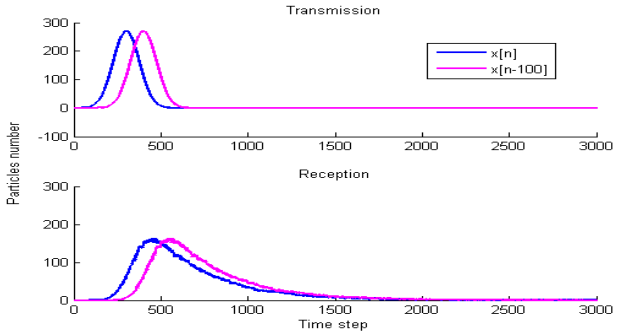

Figure 4.3: Temporal invariance validation for the single-transmitter scenario. Transmission (upper image) and reception (lower image) of two Gaussian pulses in different times.

the two independent transmission $y_3 = f(x_3) = f(x_1 + x_2) = f(x_1) + f(x_2)$.

In Fig. 4.2, the superposition principle is verified. The upper image shows the three transmitted signals: a Gaussian pulse, $x1$, a square pulse, $x2$, and the addition of both pulses, $x1 + x2$. The lower image shows the reception of these pulses at a certain distance, as well as the colored area which is the sum of the outputs as if their corresponding inputs where applied independently with respect to the channel. As the colored area matches with the output of the sum of the transmitted signals the linearity of the channel is confirmed.

In order to validate the temporal invariance, we introduce twice the same signal, but, in one is delayed with respect to the other, and we check whether the delay is maintained constant in the output of the channel.

Fig.4.3 shows the validation of the temporal invariance. The upper image shows

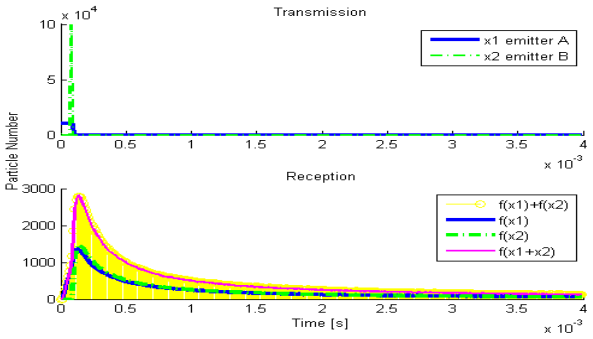

Figure 4.4: Linearity validation for the multi-transmitter scenario. Transmission (upper image) and reception (lower image) of two square pulses, one wider than the other but with the same transmitted energy.

the transmitted signals, two Gaussian pulses, one delayed with respect to the other, $x(t)$, $x(t-100)$. The lower image shows the reception of the pulses $y(t), y_2(t)$, and how the delay between the outputs matches with the delay between the corresponding inputs $y_2(t) = f(x(t-100)) = y(t-100)$.

II) Multi-transmitter scenario analysis:

We evaluate the LTI property for the two-transmitter scenario shown in Fig.4.1.b. The linearity property of this scenario is analyzed as follows: Transmitter A first transmits a signal *i.e.,* $x_1(t)$, and the output is measured $f(x_1(t))$. After that, a second transmitter, Transmitter B, transmits another signal *i.e.*, $x_2(t)$, and the output $f(x_2(t))$ is collected. Finally, both pulses are transmitted at the same time and an equidistant receiver measures the output $f(x_3(t))$. We check whether the output matches with the signal power as the sum of the two outputs corresponding to single signals transmitted independently $x_3(t) = x_1(t) + x_2(t)$.

Fig. 4.4 shows the validation of the linearity. We observe in the upper image the transmission of two different signals from transmitters A and B, a square pulse, x_1, and a spike of particles, x_2 as the narrowest possible pulse emitted, both containing the same energy. The lower image shows the reception by a receiver 500 nm away from both transmitters, $f(x_1)$,$f(x_2)$, as well as the reception of the simultaneous transmission of the two pulses, $f(x_3) = f(x_1 + x_2)$. Finally, the colored area shows

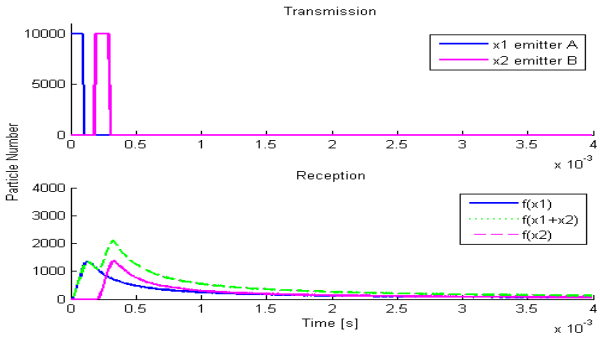

Figure 4.5: Temporal invariance validation for the multi-transmitter scenario. Transmission (upper image) and reception (lower image) of two square pulses from different emitters, in different times.

the sum of the two independent transmissions, $f(x_1) + f(x_2)$. This area matches with the received signal corresponding to the emission of both pulses simultaneously, thus confirming that the channel shows the linearity property also for the multi-transmitter case.

Secondly, to validate the temporal invariance, transmitter A releases a pulse of particles, and the transmitter B releases the same pulse delayed in time and we check if the delay is maintained in the data collected by the receiver.

In Fig. 4.5, we observe that the channel is time-invariant also for the multi-transmitter case. The upper image shows the transmitted signals x_1, x_2 emitted by both transmitters, A and B. The lower image shows the reception of each transmission, $f(x_1)$, $f(x_2)$ at a distance of 500 nm from the transmitters, and the received signal when both transmitters are transmitting simultaneously $f(x_1 + x_2)$. Again, we conclude that the delay among the transmitted pulses is the same whether or not they are transmitted simultaneously.

Assuming the channel behaves equally for the whole transmission range as it does for the tested distance, and that it behaves the same way for any number of transmitters as it does for the two-transmitter case, the channel satisfies both conditions of linearity and time invariance for both scenarios, the single-transmitter scenario and the multi-transmitter scenario.

4.2 Channel Identification Methods

4.2.1 Excitation Signals Overview

After validating the LTI property, the obtainment of the FIR model for the single-input single-output diffusion-based channel is based on choosing the appropriate stimulus. The channel must be excited in the band of frequencies where it has its important dynamics, known as the range of interest.

For a non-parametric identification approach the range of interest is not known beforehand, thus, the excitation signal must contain a rich frequency content covering the entire spectrum, such as, the Dirac Delta, or the White noise. Although these signals are theoretical signals, there are other possible excitations (approximations to broadband signals) such as: a sinus sweep, a sum of sinus, a step signal, random binary sequences, RBS, or pseudo random binary sequences, PRBS.

Utilizing a sinus sweep is very time consuming, and utilizing a sum of sinus results in a high peak factor input signal that will highly increase the noise in the receiver side. A step signal is recommended for a fast estimation of steady-state gains in the time domain and a preliminary estimation of the bandwidth magnitude, but, it is not very accurate for a characterization in the frequency domain. RBS and PRBS approximate white noise in the discrete domain, RBS are uncorrelated sequences and PRBS are periodic sequences.

For a non-parametric approach, deterministic signals are recommended because their power spectrum is constant regardless of their length [45]. Hence, PRBS seem to be the most appropriate excitation signals. Furthermore, as this study is simulation-based a Dirac delta can be approximated, by transmitting an extremely short unique pulse of particles very high in amplitude. Both methods are next detailed.

4.2.2 Impulse excitation analysis

A single impulse stimulus yields directly to obtain the impulse response and the channel transfer function is available through the Discrete Fourier Transform, DFT:

$$H[k] = DFT[h[n]] = \sum_{n=0}^{N-1} h[n] e^{-\frac{2\pi j}{N} kn}; k = 0..N-1 \tag{4.2}$$

In this communication channel the information molecules released by a nanomachine physically move according the Brownian dynamics, and they eventually reach the receiver, located at a certain distance. The propagation mean delay increases with the square of the distance, thus, this communication channel presents different impulse responses (in amplitude and in shape) for each distance. Hence, a degradation of the capacity for this channel is expected for an increase of the distance.

We simulate a transmission of a Dirac Delta by adding a punctual transmitter which transmits a high-level peak of particles instantaneously, and in order to obtain a family of impulse responses we locate the receiver at different distances, in each simulation. By taking the data proportionated by a receiver that absorbs molecules, the discrete impulse response for each distance is estimated.

After that, by computing the DFT we obtain the channel transfer function, from which we extract the Gain ($G(\omega) = \|H(j\omega)\|$), the Phase shift ($\phi(\omega) = arg(\phi(\omega))$) and/or the Group delay ($\tau_g(\omega) = -\frac{d\phi(\omega)}{d\omega}$), characterizing totally the channel in the frequency domain.

We use the receiver version that estimates the concentration by absorbing particles when they enter to its actuation space in order to obtain a homogeneous data set. This receiver model is not totally transparent to the diffusion process due to an additive concentration gradient in its actuation space can be created due to the absorption of the particles.

In order to avoid any external effect to the diffusion process, we follow a second approach, that can be used for any signal excitation, based on the definition of the channel transfer function as the relation in frequency of any output with respect to

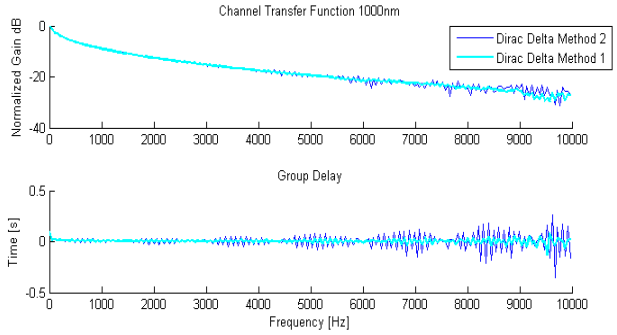

Figure 4.6: Comparison of the Channel Transfer Function for a distance of $1\mu m$ obtained by placing a transparent receiver (bright blue) or a receiver that absorbs the particles (dark blue). The Upper image shows the normalized gain and the lower image the group delay, both up to 10Khz.

the input as:

$$H(j\omega) = \frac{Y(j\omega)}{X(j\omega)} \tag{4.3}$$

We simulate the transmission of a concentration sequence with a transmitter that forces a concentration in its actuation space, C_{in}, and the output concentration is measured by collecting the number of particles measured by a transparent receiver located at a certain distance, N_p, and dividing it into its actuation space, obtaining C_{out} . By locating a receiver in each distance, and transforming all the signals to the frequency domain, we obtain a family of channel transfer functions as follows:

$$H(j\omega, d) = \frac{C_{out}(j\omega, d)}{C_{in}(j\omega, d)} \tag{4.4}$$

And a family of impulse responses:

$$h(t, d) = DFT^{-1}[H(j\omega, d)] \tag{4.5}$$

.

As an example, fig.4.6 shows the obtained results for a distance of 1000nm by means of the two mentioned methods, in both cases using as excitation signal the Dirac Delta approximation. The upper image shows the channel attenuation and the lower image shows the group delay. As we can see both approaches lead to the same

results, hence, we can consider negligible the extra concentration gradient added by a receiver that absorbs particles.

4.2.3 PRBS excitation analysis

PRBS are a two levels signals composed of a succession of pulses modulated in its width, approaching the rich content of frequencies of the white noise [12].
These sequences are characterized by 4 parameters:

1. The signal amplitude levels.
2. The length of one period.
3. The clock period, T_{gen}, which determines the minimum possible width and so the spectral properties of the sequence.
4. The number of periods to transmit, N_T. By increasing the number of periods more accurate the results are.

In order to generate an adequate PRBS (to cover the range of interest) some care is required in the election of T_{gen}:

- A PRBS has enough power (constant power spectrum) for approximately $\frac{0.45}{T_{gen}}$ [36], thus, according to the range of interest of the channel, characterized by the maximum frequency f_{max}, the clock period has to be chosen as: $T_{gen} = \frac{0.45}{f_{max}}$.

As an example Fig. 4.7.a shows a PRBS generated to cover the identification process from the low frequency range up to $10Khz$, thus, f_{gen} is equal to $22.22Khz$ (or $T_{gen} = 0.45\mu s$). The temporal length is $0.0248s$ (only one period is shown). The amplitude levels, max/min values are equal to 350 and 700 particles, chosen to cover the evaluation distance with a satisfactory signal to noise ratio, SNR.
Fig. 4.7.b shows the power spectral density of the generated sequence, where we see that up to $10KHz$ (marked off red), the spectrum is flat.
Fig. 4.7.c shows the autocorrelation function Γ_{xx}, where we see the uncorrelation property, the maximum of the function requires to displace the sequence an interval

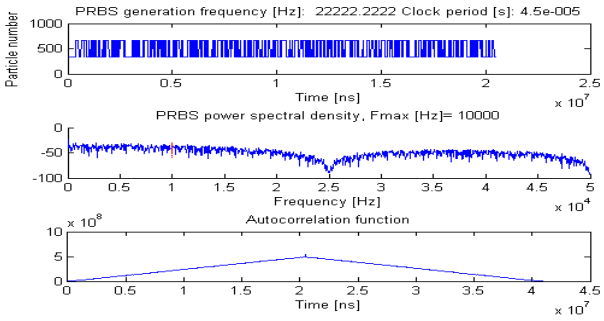

Figure 4.7: a) PRBS; b) Power Spectral density; c) Autocorrelation function.

equal to the length of the sequence.

In order to identify the channel with a PRBS, we simulate a transmitter that encodes the information into the molecule concentration imposed over its actuation space $C_{in}(t) = PRBS$, and a transparent receiver estimates the output concentration by measuring the number of particles over its actuation space, $C_{out}(t)$.

The Wiener-Hopf equation relates the autocorrelation function of the input signal Γ_{xx}, with the cross-correlation of the input/output signal Γ_{xy} and the impulse response, it is defined [48] as follows:

$$\Gamma_{xy}(\tau) = \int_0^\infty h(\tau)\Gamma_{xx}(t-\tau) \tag{4.6}$$

Working in the frequency domain, the Wiener-Hopf equation is defined as:

$$S_{xy}(j\omega) = H(j\omega)S_{xx}(j\omega) \tag{4.7}$$

where $S_{xy}(j\omega)$ is the cross-power spectral density, $S_{xx}(j\omega)$ is the input power spectral density and $H(j\omega)$ is the channel transfer function.

The channel transfer function is computed by measuring the output of the channel for any distance, computing the cross-power spectral density between the input signal PRBS and the output of each receiver, the power spectral density of the input and applying the previous formula (4.7).

We have approached the identification process by following two alternatives, using as excitation signal a Dirac Delta approximation or using a PRBS. Both approaches

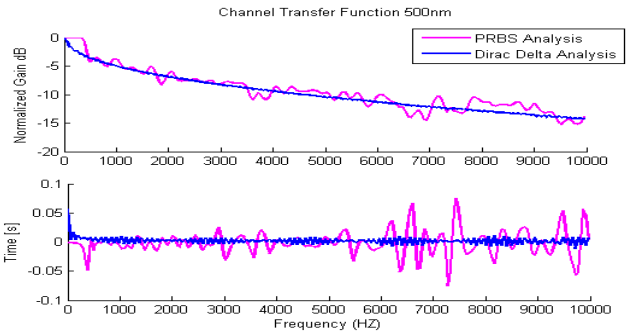

Figure 4.8: Comparison of the Channel Transfer Function at a distance of 500nm and up to 10KHz, obtained by exciting the channel with a PRBS (magenta) or by using the impulse as excitation signal (blue). Upper image shows the normalized gain, lower image shows the group delay.

are valid. Fig.4.8 shows an example of the obtained results of the channel transfer function for a distance of 500nm by means of both methods. The blue curves correspond to the impulse analysis using a transparent receiver and the magenta curves correspond to the PRBS analysis. The upper image shows the normalized gain, and the lower image shows the group delay.

The PRBS analysis leads to results that own higher fluctuations for any distance, thus, this method results on less accurate results, hence, from this point on, the shown results were obtained by the Dirac Delta analysis.

4.3 Channel Identification Results

This section presents the channel transfer function and the channel impulse response obtained for different scenarios of a diffusion-based communication channel.

4.3.1 Normal Diffusion-based Channel

In a normal diffusion-based communication channel, as it is mentioned in previous sections, the spread of a net flux of particles upon a concentration gradient is modeled by the first Fick's law and the distribution of particles in the space is well defined by the second Fick's law.

I) 3-D space Impulse Response

The impulse response displayed in fig.4.9.a. is obtained for calcium particles (r=0.2nm) immersed in cytoplasm fluid in a 3-dimension space for a transmission range of $0 - 2\mu m$ through *N3Sim*.

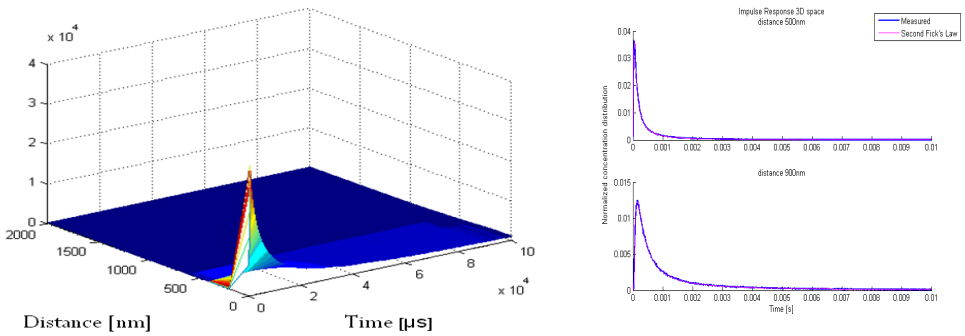

Figure 4.9: a) Impulse response of a 3-D space for the transmission range: $0 - 2\mu m$, b) Validation for the obtained impulse responses by comparison between the solution of the second Fick's Law (magenta) to the simulator output (blue). Upper image: 500nm, lower image: 900nm

The correct behavior of the simulator for the normal diffusion-based channel is validated by comparing the measured distribution of concentration in the space as the result of transmitting a spike of particles, to the analytical curves obtained by means of computing the solution of the second Fick's law.

Fig. 4.9.b upper and lower images show that the measured impulse responses coincide with the curves obtained by means of the diffusion equation solution, both normalized, for a distance of 500nm and 900nm respectively.
We see how the width of the impulse response increases with distance. It reflects that any transmitted signal will suffer a widening that will increase with distance. The inverse of the temporal duration of the impulse response approximates the bandwidth of the channel, hence, it decreases with distance.

II) 3-D space Channel Transfer Function

The channel transfer function displayed in fig. 4.10 is obtained for calcium particles (r=0.2nm) immersed in cytoplasm fluid in a 3-dimension space. Fig.4.10.a shows the normalized Gain of the communication channel and fig. 4.10.b the group delay, both for a frequency range of: $0-10Khz$ and a transmission range of $100-1000nm$.

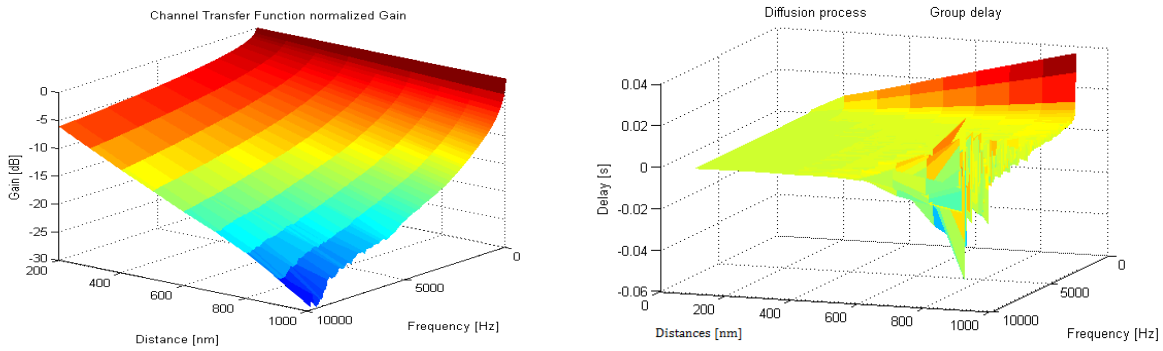

Figure 4.10: a)Normalized Gain up to 10 KHz for a transmission range of: $0-1\mu m$
b) Group delay up to 10 KHz for a transmission range of: $0-1\mu m$.

The obtained normalized gain shows that for any distance the channel presents a low pass filter behavior, attenuation increases with frequency. The group delay (delay that a signal experiences during the propagation from the transmitter to the receiver as a function of the frequency) increases with the distance for the low frequency range. Furthermore, the images shows that fluctuations appear for large distances in the high frequency range. These unwanted perturbations are related

to perturbations in the estimated concentration by the receiver located at larger distances, where, the SNR is very poor.

The diffusion process is mainly characterized by the diffusion coefficient D, which includes all the information from the environment and the diffusion process (fluid viscosity, temperature, and diffusing particles nature). It specifies how fast the diffusion process is. The higher the value of the diffusion coefficient, the faster the diffusion process. Hence for diffusion scenarios with high D values, the attenuation will be lower and the bandwidth will be wider.

III) 2-D space Channel Transfer Function

In order to compare the normal diffusion-based channel's behavior to the anomalous diffusion channel's behavior in terms of channel transfer function, as *N3Sim* allows to simulate interactions amongst particles only for a 2-D space, we represent also the results of the normal diffusion based channel for calcium particles in cytoplasm obtained for a 2-D space. Fig.4.11 shows the channel transfer function in terms of normalized gain, group delay and nyquist plot, obtained for a unique distance, e.g., 500nm.

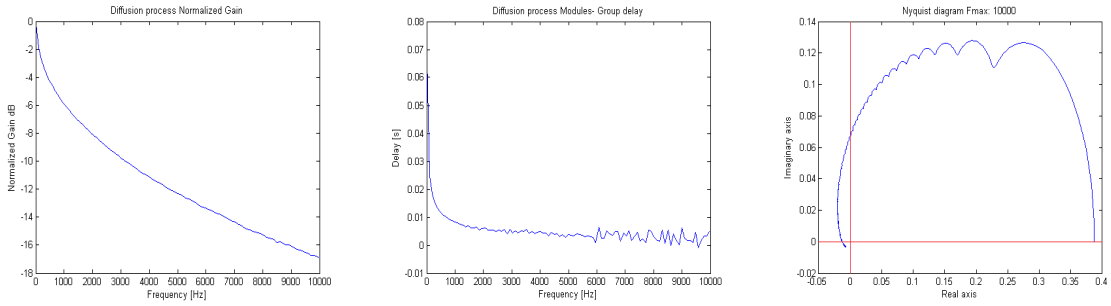

Figure 4.11: a)Normalized Gain for 500nm up to 10KHz b)Group delay for 500nm up to 10KHz c) Nyquist diagram for 500nm up to 10KHz.

The results are represented for the frequency range of $0 - 10KHz$. Fig.4.11.a shows the normalized gain, fig.4.11.b the group delay and fig. 4.11.c the nyquist diagram. In the nyquist diagram, the imaginary part of the channel transfer function is plotted

versus the real part in polar coordinates, including magnitude and phase information in an only figure.

The Nyquist plot provides stability information for channels or systems containing time delay. The peaks we observe in the nyquist plot are the result of the delay between input/output. The magnitude is the distance from the origin to any point and the phase is the angle. The curve shows that the phase suffers three changes of 90 degrees, which means the characteristic equation of the channel at this distance adds three real poles.

4.3.2 Anomalous Diffusion based channel

The anomalous diffusion-based channel covers all possible diffusion-based scenarios where Fick's Law are not applicable. Several possibilities can change the normal diffusion process: elastic collisions, electrostatic interactions, obstacles in the communication scenario, ot the nature of the fluid allowing the diffusing particles to add some inertia.

Up to know we have focused the analysis for the diffusion of calcium particles in cytoplasm, mainly conformed of water molecules ($D_{cytoplasm} = 1^{-9}$). We consider the particle's interactions as elastic collisions, electrostatic forces are not taken into account in this analysis.

The water molecule radio is equal to $r = 0.1nm$ and the calcium particle radio is equal to $r = 0.2nm$. Due to their sizes are almost the same, the effect two calcium particles colliding is almost the same as when a calcium particle collides with a water molecule, hence collisions do not change the diffusion process and the mix behaves as an ideal mix (see. Fig.4.12.a that shows the same reception process when interactions are activated (green) and where are not (blue)).

For higher sizes of diffusing particles the effect produced by the elastic collisions is not longer negligible (see Fig.4.12.b that shows different reception processes when interactions are activated (green) or not (blue). The figure shows that the propagation is faster due to the collisions between the particles.)

We have obtained that elastic collisions change the diffusion process, and that their

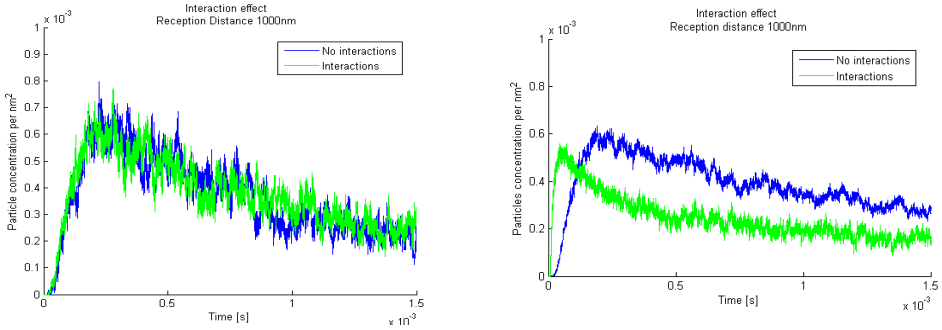

Figure 4.12: a) Interaction effect for calcium particles immersed in cytoplasm b) Interaction effect for bigger diffusing particles immersed in cytoplasm.

effect is more visible when the difference between the size (mass) among the diffusing particles and the ones from the fluid increases.

Although the diffusion process when modeling the collisions is different (anomalous diffusion), the channel's behavior for the single-transmitter scenario is still linear and time invariant (the analysis done in Section 4.1.1 for this diffusion scenario verifies it), however, for the multi-transmitter scenario the results show the channel is no longer linear. (see Section 6.2).

Another scenario in which anomalous diffusion takes place is when the fluid's nature allows the diffusing particles to add inertia to their trajectory. With *N3Sim*, different impulse responses are obtained according to different values of the inertia factor. An initial radial velocity applied to the particles by the transmitter nanomachine is added to the simulations, which intensifies the visibility of the inertial effect.

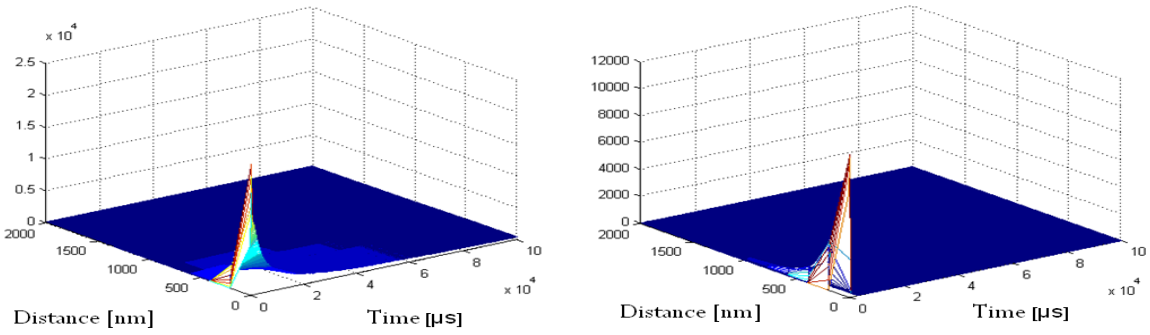

Figure 4.13: Impulse responses for anomalous diffusion for a transmission range of: $0 - 2\mu m$. a) Inertia factor equal to 0.4 b) Inertia factor equal to1.

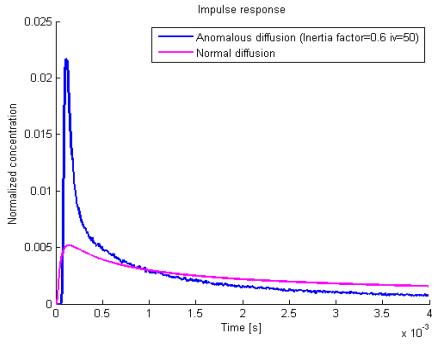

Figure 4.14: Comparison of impulse response for the distance 500nm for a specific case of anomalous diffusion and for normal diffusion

Fig.4.13, shows the effect of adding inertia to the impulse response of the diffusion-based communication channel, left image corresponds to an anomalous diffusion where the transmitter initiates the diffusion process by applying a radial velocity of $50\frac{nm}{ns}$ and the previous velocity is kept according to an inertial factor value equal to 0.4, and the right image corresponds to the anomalous diffusion where the previous velocity is totally maintained, thus the inertia factor is 1. When the inertia factor is increased the randomness of the movement is decreased, and the concentration is spread in space in a faster way, allowing faster communication links.

I) 2-D space Impulse response

In order to compare the behavior of the anomalous diffusion-based channel with the normal diffusion-based channel in terms of gain, group delay and nyquist plot, we chose a specific case of anomalous diffusion which corresponds to an inertia factor equal to 0.9. and an initial velocity of $50\frac{nm}{ns}$.
Fig.4.14 shows the difference in the impulse response of both channels for a distance of 500nm.

II) 2-D space Channel Transfer Function

The channel transfer function for the anomalous diffusion-based channel scenario just mentioned, is displayed in fig.4.15.

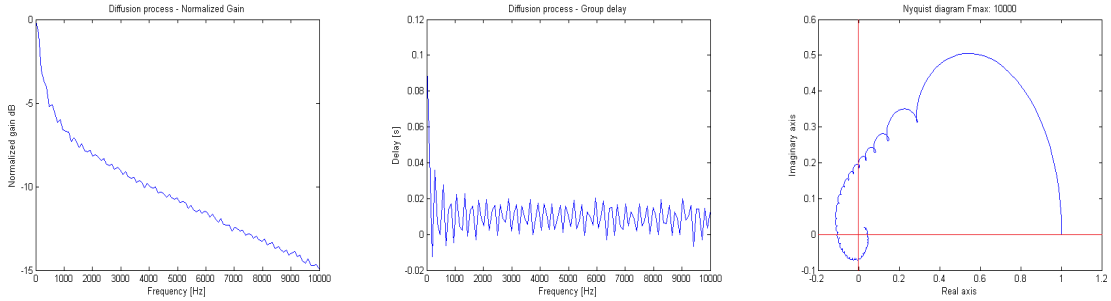

Figure 4.15: a)Normalized Gain for 500nm up to 10KHz b)Group delay for 500nm up to 10KHz c) Nyquist diagram for 500nm up to 10KHz.

The results are for the frequency range $0 - 10KHz$. Fig.4.15.a shows the normalized gain, anomalous diffusion-based channel shows less attenuation than the normal diffusion-based one. Fig.4.15.b shows the group delay, which experiences much more fluctuations than in the normal diffusion. Fig. 4.11.c shows the Nyquist diagram, where we see the peaks produced by the delay between the input and the output are more pronounced. It shows the gain for low frequencies is zero and decreases rapidly, and it shows the phase suffers four changes of 90 degrees in contrast to the normal diffusion channel that suffers 3 changes.

4.4 Dispersive channels

In a diffusion-based communication channel, a transmitted signal encoded into the number of transmitted particles or into the molecule concentration, suffers a distortion in shape (widening) which increases with distance. This effect can be observed in Fig. 4.4 lower image, which shows the reception of the upper image pulses, where the reception wide is longer than the original.
This widening is explained from the microscopic point of view of the diffusion process as follows:

- The transmitted signal is composed by a number of discrete particles, each one propagates independently by following the Brownian dynamics, thus there is not a wavefront traveling at a constant velocity as in the case of EM trans-

missions. In diffusion-based communications, transportation delay scales as square of the distance, thus the average propagation velocity decreases with distance. This effect produces a shape-widening of any transmitted signal measured at a certain distance, observable as an addition of a long tail that follows an exponential decay, slower exponential decay for further distances.

The dispersion phenomenon a signal suffers when it passes through a dispersive channel in EM communication may be compared to this phenomenon, due to in both cases the shape of the transmitted signal, is distorted.

Dispersive, is a non linear feature that causes changes in the shape of the transmitted waveform. There are different types of dispersion in traditional communication channels:

- Time dispersion: it is produced by the multipath effect. The received signal is the sum of different versions of the transmitted signal arriving through different paths. This effect is consequence of multiple reflections.

  This dispersion is common in some communication channel e.g., indoor wireless channels. Despite it is a non linear feature the time dispersive channels are modeled as linear channels, in which the impulse response is modeled as the addition of several contributions:

$$h(\tau) = \sum_{\mu=1}^{M} h_\mu d(\tau - \tau_\mu) \tag{4.8}$$

  where h_μ is the attenuation related to each path.

  In the diffusion-based channel, the widening or dispersion effect is not possible to be related to the multipath effect due to the signal is already a contribution of single particles, being each one independent.

- Chromatic dispersion: it causes the spatial separation of the wavelengths components of the transmitted signal, and the group velocity becomes frequency-dependent, thus each wavelength travels at a different velocity. It is present in optical transmissions. This dispersion causes a shape-widening which increases proportionally to the transmission distance.

In the diffusion-based channel the shape-widening occurs at a rate proportional to the square of the distance [22], thus, the widening in diffusion-based channel is more pronounced than in a optical channel.

- Frequency dispersion: it is associated to a time varying channel gain of the channel. This kind of dispersion is present in channels where the distance emitter/receiver changes, producing a frequency shift on the received signal. Diffusion-based communication channel does not changes its spectral properties over time.

The widening phenomenon that appears in the diffusion-based channel is a different effect than the widening produced by any of the mentioned dispersive channels, and it is consequence of the diffusion process characteristics themselves.

4.5 Molecular Signaling

In a diffusion-based molecular channel, a transmitter nanomachine is envisioned to encode the information by releasing particles to the medium following a release pattern, thus causing a variation of its local concentration, which propagates throughout the medium. A receiver nanomachine estimates the concentration of molecules in its neighborhood and, from this measurement, recovers the release pattern decoding the transmitted information.

In [40] a different encoding technique is proposed. The communication scenario contains a high homogeneous concentration of particles in the space before any transmission and the particle emission process, involves the increase or decrease of the particle concentration rate in the environment according to a modulating input signal. The concentration rate is propagated throughout the medium and a receiver decodes the information by measuring the concentration and evaluating the incoming concentration rate, recovering the transmitted modulating signal.

According to our vision of the transmission process, the communication over the diffusion-based channel requires that all transmitted signals assume non-negative values. In this section, we give guidelines on the necessary transmitted power to

reach a specific distance with the minimum Signal to Noise Ration, SNR, that allows a receiver to recover the signal.

Assuming that the available number of particles to transmit by a nanomachine is the energy, and, the total number of transmitted particles is the transmitted power, this section shows how the overall transmitted power is distributed in the space, and from this curves, the minimum required transmitted power to reach a distance is assessed.

4.5.1 Path loss curve

The path loss curve defines how the transmitted power is spread over space, in this section it is analyzed as the variation of the overall received power over the communication space.

This evaluation is done by transmitting a spike of particles in a 2D space and measuring the total received power for a short transmission range spanning distances from 100nm to 1000nm, by collecting the concentration estimated by several transparent receivers (with radius equal to 100nm) located all over the space.

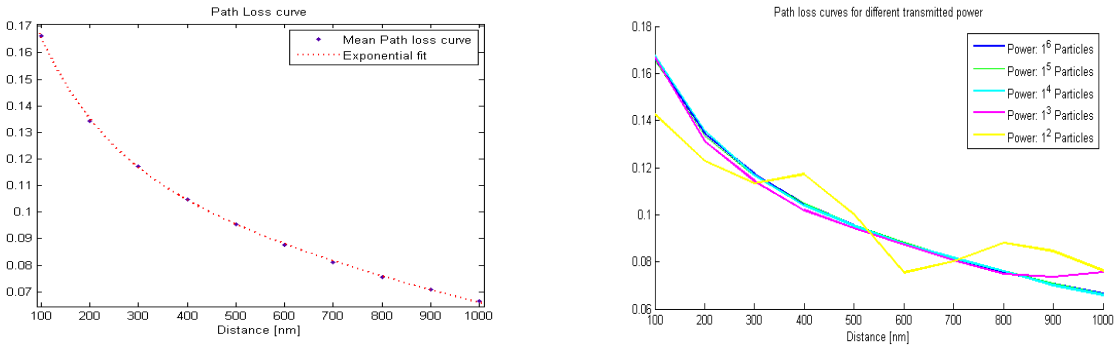

Figure 4.16: a) Path loss curve for the transmission range: $100nm - 1\mu m$ and its best fitting curve b) comparison of path loss curves for different transmitted power quantities.

Fig.4.16.a shows the path loss curve, and its best fitting curve, which corresponds to a sum of two exponentials (obtained for a root means square error of $rmse = 0.0005$) equal to:

$$f(x) = 0.091e^{-0.0075x} + 0.132e^{-0.0007x} \tag{4.9}$$

Distance [nm]	**200**	**400**	**600**	**800**	**1000**
Power $[N_p]$	**500**	**1000**	**5000**	**10000**	**50000**

Table 4.1: Minimum power, in number of particles, to reach a distance

being x the distance between the transmitter to the receiver.

We simulate the same communication scenario for different transmitted power values, in order to find the necessary transmitted power to reach satisfactorily any distance. When the transmission is done with enough power, the power energy distribution follows the previous curve, otherwise the path loss curve goes off.

Fig.4.16.b shows the results of the path loss curve for different orders of magnitude of transmitted power. We can see how when the transmitted power is equal to 1000 particles, the curve goes off the course at distances 900 and 1000nm, which indicates that this transmitted power is not enough to excite these distances. The graph shows that for a transmission of 100 particles, the obtained curve does not fit with the rest at any distance, due to the received power is extremely low.

Table.4.1 shows orientation values in number of particles needed to reach a distance in a diffusion-based 2-D space channel. It is important that, the particles number correspond to the total power per transmitted symbol, as we used spikes they coincide with the amplitude, but if we use wider pulses, it correspond to the total power per pulse.

Furthermore, it is important to notice that bigger the receiver higher is the estimated concentration and lower is the needed transmitted number of particles. This evaluation is done for small receivers (r=100nm) and for the short transmission range of 100-1000nm, but they are equally valid for a transmission range of $1 - 10\mu m$ if receivers of dimensions (r=$1\mu m$) are placed.

4.5.2 Environmental sensibility

The transmission of information is based on the diffusion of molecules through the medium. The factors that condition how the diffusion process is, are:

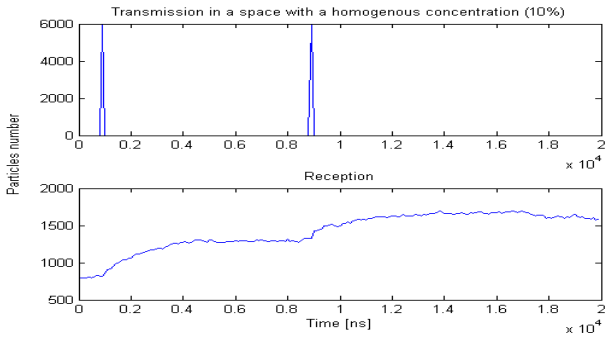

Figure 4.17: Transmission and reception in a diffusion-based communication scenario containing a high homogeneous concentration of particles, which corresponds to the 10% of the total simulation space at a distance of 200nm

- The medium. The higher its viscosity, the slower the diffusion process. Furthermore, obstacles in the medium slow down the diffusion process.

- Temperature. The higher the temperature, the faster the diffusion process.

- Diffusing particle sizes. The higher its radius, the slower the diffusion process.

- Ration amongst size of diffusing particles with respect to the fluid particles. For a low ratio value, diffusion process is slower than it should be according to the diffusion coefficient and collisions effects are negligible, however, for a high ratio value, the diffusion coefficient is well defined and collisions have more effect in the propagation process.

- The presence of an homogeneous concentration in the communication scenario. It increases the received noise power, and in case its value is very high, it makes difficult the exchange of information, and more energy is required to be transmitted per symbol.
  Fig.4.17 shows this effect.

The simulation (fig.4.17) is done by placing a transmitter and a receiver at a distance of 200nm, in a bounded space of $1\mu m$ per $1\mu m$, which simulates an infinite space. Fig.4.17 upper image shows the transmission of two spikes (6.000 particles peak level) and fig.4.17 lower image shows the reception process, in which, we see the transmission information could be hardly recovered due to the medium contains a

high concentration of particles. Background concentration in this example is formed by 625.000 particles.

In the diffusion-scenario introduced at the beginning of this section, [40], the homogeneous concentration makes possible the communication and does not increase the noise in the receiver side, due to the recovered information is the concentration rate.

Chapter 5

Modulation Schemes Comparison

The goal of this chapter is to compare and analyze different modulation schemes in order to find the one with the best performance in terms of communication over the diffusion-based communication channel for molecular nanonetworks.

5.1 Introduction

We compare different modulation schemes with the results from *N3Sim*. In a diffusion-based communication channel, simple modulation schemes are required, since the transmission of information requires the physical transportation of molecules, which is a slow process. Moreover, biological nanomachies are expected to be simple machines with limited computing capabilities.
The modulation schemes used in EM communication can be classified according to the presence or not of carrier signal:

- In carrier-based modulations schemes, common in traditional narrow-band communication systems, the digital stream of bits is translated to the high part of the spectrum before transmitting. The information is transmitted by changing parameters of the carrier signal, e.g. its frequency or its phase.

- In pulse-based modulation schemes, proposed for Impulse Radio Ultra-Wide-Band (IR-UWB) systems, the information is transmitted without a carrier,

based band pulses are directly radiated. IR-UWB communicates by transmitting and receiving extremely short pulses with long time slots among them. This technique includes an orthogonal time hopping as a synchronous medium access technique, in order to allow multi-transmission during one time slot [49], thus increasing the throughput of the network.

Pulse-based modulations schemes present some advantages with respect to continuous carrier-based modulations schemes, such as:

1. Simplicity, since there is no carrier synchronization overhead.
2. Higher peak output level for an available power, allowing:
   - Better noise performance
   - Longer transmitting distances
3. Bio-compatibility. Both intra and inter communication processes in cells are done by means of exchange of pulse sequences. For instance, neurons in the central nervous system communicate through the generation of stereotyped pulses, termed action potentials or spikes [13].

5.2 Pulse-based Modulation Techniques

In order to find the pulse-based modulation scheme that best suits in the diffusion-based molecular communication channel, a preliminary analysis is done in order to find the pulse shape that experiences a better performance while passing through the channel, to use it as the basis for any pulse-based modulation scheme.

5.2.1 Pulse shaping

Pulse shaping is the analysis done to find the pulse that best keeps its original shape in the reception side, allowing to reduce inter symbol interferences, ISI.
In traditional communications, in order to avoid ISI, the transmitted pulses must satisfy the Nyquist Criterion (pulse equals zero at the ideal sampling times associated

with past or future symbols), such as the rectangular pulse or the root cosine pulse. Despite this criterion, IR-UWB uses the first derivative of the Gaussian pulse, known as monocycle, due to its simplicity to be transmitted by the radiating antennas used in IR-UWB systems.

As it is explained in Section 4.4, in the diffusion-based channel the transmitted signal shape is always distorted by the addition of a long tail in form of exponential decay. The widening of the pulse is inevitable and distance-dependent. Furthermore, it limits the maximum achievable bandwidth for each distance.

Since the diffusion-based channel only allows the transmission of low-bandwidth signals, behaving as a low pass filter, we compare the performance of three basic pulses (a square pulse, a cosinus pulse and a guassian pulse) according to their different spectral properties.

For a limited transmission width, the square pulse has its spectral components the most widespread, the energy is spread on the sides lobes of its spectrum. In order to suppress this energy spread, the temporal sharp edges of the square pulse can be rounded, obtaining a cosinus pulse. Cosinus pulse also presents sides lobes but with less energy. Finally, the gaussian shows the most compacted spectrum.

The definition of these pulses in time and frequency is shown in the following lines:

1. **Square Pulse**. Defined in time as: $r(t) = \text{cte}; -\frac{T}{2} < t < \frac{T}{2}$
   Defined in frequency as: $R(f) = \frac{T \sin(\pi f t)}{\pi f t}$

2. **Cosinus Pulse**. Defined in time as: $\cos(\frac{2\pi t f_a}{2}); -\frac{1}{2f_a} < t < \frac{1}{2f_a}$

   Defined in frequency as: $C(f) = \frac{\cos(\pi \frac{f}{f_a})}{1 - (2\frac{f}{f_a})^2}$

3. **Gaussian Pulse**. Defined in time as: $g(t) = e^{-t^2/2u^2}$;being $u = 1/2\pi f_b$.
   Defined in frequency as: $G(f) = e^{-(2\pi f u)^2}$

Two parameters are constrained in transmission, the pulse-width and the power. This allows to compare the different pulse-shapes under the same conditions in

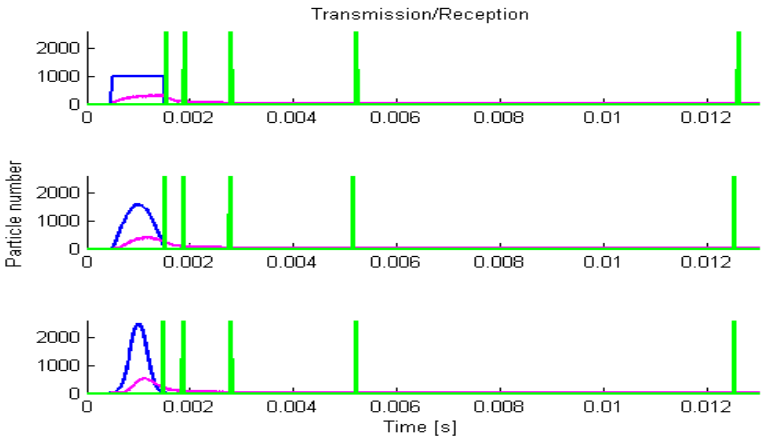

Figure 5.1: Square (a), cosine (b) and Gaussian (b) pulses transmission/reception processes.

terms of:

- Widening factor.
- Received peak value.
- Received total power.

The optimal pulse shape is the most unaltered (minor widening), allowing the maximum bandwidth, and minimizing the needed transmitted power for a specific distance.

Fig. 5.1 shows the transmission and reception of the three previously defined pulses, for a transmission range of 400 nm. The green vertical lines correspond to the time instants when the received signal owns the 50%, 60%, 70%, 80% and 90% of the total received power, from left to right, respectively.

- We observe that all the received pulses have a long tail and they are therefore distorted, albeit with a different degree of distortion. The Gaussian pulse (in the third image) shows the least amount of distortion, while the square one (in the first image) is the most distorted one. This result was expected due to the spectral properties of the pulses mentioned before and the LPF channel's behavior.

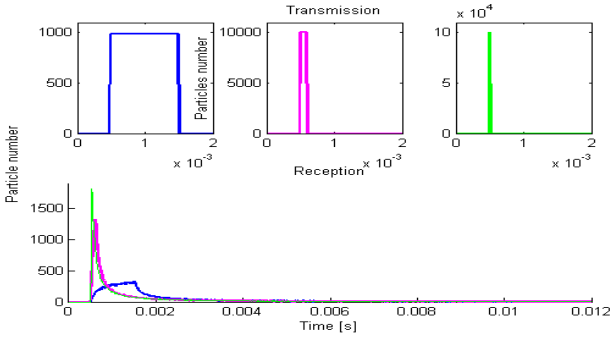

Figure 5.2: Transmission (a) and reception (b) of square pulses with the same energy and different time durations.

- The maximum received peak level is obtained for the reception of the Gaussian pulse (501). The peak value for the reception of the square pulse is equal to 316 and to 410 for the reception of the cosinus pulse.

- The vertical lines in Fig. 5.1 show that the received power distribution of the received pulses has almost no dependence on the pulse shape.

In conclusion, for a pulse transmission constrained in its power and in the time duration, the Gaussian shape yields to the best performance, even though the differences with other shapes are minimal.

As we have observed the pulse shape for the diffusion-based communication channel is not an important parameter. However, we extract from this analysis that for a given constrained power, the more compacted the transmission is, the higher the peak value of the received signal is. Furthermore, we find that the widening of the pulses in reception is what limits the maximum achievable rate of transmission. The shortest the pulses in transmission, the better the performance is. Therefore, the optimal pulse shape is a spike pulse (approximation to the Dirac delta).

Fig. 5.2 shows this effect. The upper side of Fig.5.2 shows the transmitted square pulses, all of them with the same energy but having different lengths. The lower image shows the three receptions; where we observe that the minimum width corresponds to the case of transmitting the shortest square pulse.

Last, we analyze how the power is distributed in time in the reception side for any transmission distance of a spike pulse and we evaluate the time instants for receiv-

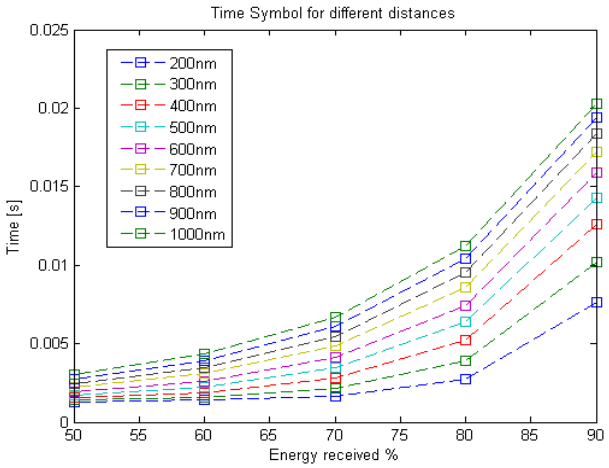

Figure 5.3: Time interval for different percentages of received power and for several distances, the transmission distance ranges from 200 nm to 1000 nm.

Received percentage of power]	**90%**	**80%**	**70%**	**60%**	**50%**
Time interval [s]	**0.0201**	**0.0113**	**0.0068**	**0.0044**	**0.003**

Table 5.1: Time interval for a receiver located 1000nm away from the transmitter to receive part of the transmitter power

ing the 50% of the total energy 60% 70% 80% and 90%. Fig. 5.3 shows these time intervals for different distances. Table 5.1 shows the time interval for a distance of 1000nm, as an example.

5.2.2 Analytical Comparison

To transmit information over the diffusion-based communication channel a train of pulses (spikes) is needed, to encode the information in some parameter of the train. Any transmitted particle sequence can be mathematically described by the following expression:

$$s(t) = \sum_{-\infty}^{\infty} (\alpha_i[n](\varphi_i[t - nT]); \tag{5.1}$$

where α_i corresponds to the symbols, and φ to the basis.

Inter symbol interferences prevent a receiver to recover the transmitted information. In order to avoid this effect, a guard time between symbols needs to be added in

transmission. The symbol time, T_s, will be the sum of the symbol length (as the pulse is a spike, it is almost negligible) and the guard time. The guard time can be adjusted by the transmitter to reach any distance with the required ISI value. By increasing the guard time the ISI decreases but also the available bandwidth decreases, hence, a trade-off between increasing the rate (decreasing the symbol time) while increasing ISI in reception has to be reach.
Information can be encoded by changing different parameters of the pulse train:

- The amplitude of the pulse, (Pulse Amplitude Modulation, PAM).
- The width of the pulse (Pulse Width Modulation, PWM).
- The pulse position within the symbol time interval (Pulse Position Modulation, PPM).
- The time between pulses, obtaining a variable symbol time (Pulse Interval Modulation, PIM).
- The pulse transmission rate (Rate Modulation, RM).

The PWM scheme is disregarded due to the information is encoded into the width of the transmitted pulses, parameter that must be kept as shorter as possible in order to reach the maximum bandwidth.
A new paradigm scheme which belongs to the PIM family, called Communication through Silence, CtS, introduced in [50] is analyzed and compare to the PAM, PPM and RM performances.
In order to evaluate and compare the different pulse-based modulation schemes, we simulate the transmission of a specific bit sequence encoded and transmitted in the binary versions of PAM and PPM modulation schemes, and M-symbol (M=32) version of CtS and RM.
We analyze and compare the following parameters for each modulation scheme:

- ISI, in terms of Peak to Peak value, P-P.
- Energy per bit, E_b or transmission range.

- Throughput, R.

We analyze the four proposed schemes in an analytical way:

- Using On-Off Keying (binary PAM version), a digital '1' is transmitted by sending a spike, and a '0' by silence. All the available energy per symbol is utilized for the transmission of the '1'. The receiver decodes the information just by sensing the environment in its actuation area. When the measured concentration exceeds a threshold, the received symbol is understood as a logical '1'; otherwise, it is understood as a '0'. This communication scheme seems, a priori, very suitable for this communication channel, where simplicity is required, and it allows asynchronous communication. A good management of the available power in transmission is done, thus increasing the transmission range (very limited in this communication alternative).

- Using PPM, a digital '1' is transmitted by sending a spike in the first half of the time symbol T_s, and a digital '0' by sending a spike during the second half of the T_s. The receiver decodes the information by sensing the concentration in its environment, but some synchronization among transmitter/receiver is required in order to decode the information as a '1' or a '0' according to the position of the received pulse within the T_s interval. This communication scheme seems, a priori, less suitable for this communication channel, since the energy per symbol is divided into the transmission of two pulses, limiting the coverage distance.

- Communication through Silence, CtS, uses time as a new dimension to encode the information. This modulation scheme proposes to encode a entire bit stream in a transmission of two pulses. A transmission of a first spike is needed as a preamble bit (start pulse), and a last spike is needed in order to finish the transmission (stop pulse). For instance, by using the 2^7 symbol version, the bit stream (1100001) which corresponds to the symbol (decimal value) '97', is directly encoded in the time between the two spikes. The benefit comes from using silence to transmit the symbol, which reduces the number of pulses to

be transmitted. This results in a improvement in the energy consumption, which can be, a priori, an improvement on the achievable bandwidth. The receiver decodes the information by sensing the environment. When it detects a pulse, it starts counting until receiving the following pulse. The decoded information corresponds to the counting value for the reception of the second pulse. This communication scheme requires synchronization, receiver and transmitter sharing a common clock.

- In Rate modulation, the information is encoded into the rate of transmitting the spikes. This technique is also used by the nervous system by sending trains of action potentials. The rate of transmitting the spikes is related to the stimulus that is being received. When the stimulus is poor, the train has a low frequency, and when the stimulus increases the rate increases. The receiver decodes the information by measuring the average number of action-potentials per unit time. We evaluate this scheme by transforming a burst of bits from the bit stream to decimal values in order to use it as an M-symbol modulation scheme. A priori, this modulation scheme is highly inefficient in terms of energy because it is based on transmitting a train of spikes per symbol. In consequence, the maximum achievable bandwidth seems lower than with the other commented schemes. However, in [16] it is said to be a robust modulation scheme with respect to the irregular inter-spike interval noise, present in nervous system communication. Due to this feature, we analyze it as an alternative for the diffusion-based channel to obtain robust communication links.

5.2.3 Simulation-based Comparison

The comparison is done by using the bit stream “0110110001” as reference.
On the one hand, OOK is compared to PPM, using ISI ($P - P$) and transmission range as evaluation metrics, for a constrained in transmission in energy per symbol, E_s and symbol duration T_s. Since T_s determines the maximum achievable rate, in this comparison, the bandwidth is predetermined by the transmitter nanomachine.

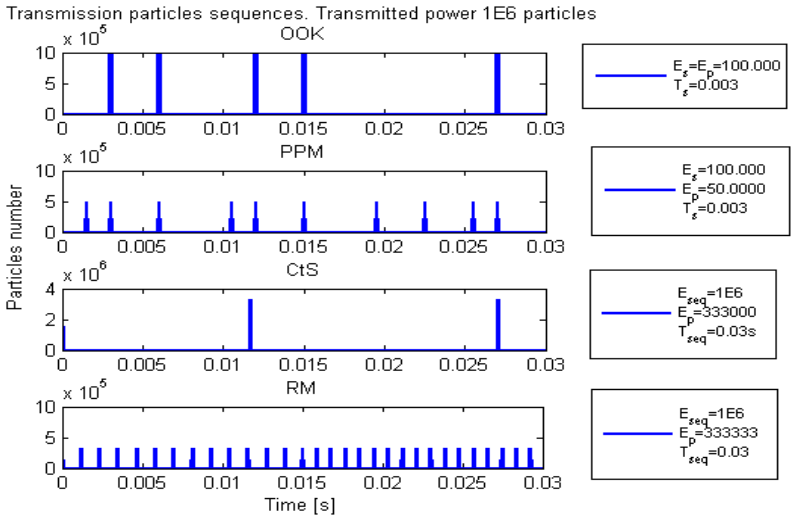

Figure 5.4: Transmission process for OOK, PPM, CtS and RM. (E_s= energy per symbol, E_p= energy per pulse, T_s= time per symbol, E_{seq}= energy per sequence, T_{seq}= time per sequence.)

Furthermore, they are compared using throughput, R, and E_s as the evaluation metrics, for a transmission without constrains.

On the other hand, CtS is compared to RM using ISI ($P - P$) as metric, by using their 32-symbol modulation versions (five bits per symbol), thus, transmitting the previous bit stream encoded as a sequence of two symbols "13, 17". A constrained in transmission is done in order to compare them under the same conditions, in the overall energy (energy per sequence, E_{seq}), and in the total time of the transmission (sequence duration T_{seq}).

Fig.5.4 shows the transmitted signals encoded according to each scheme (OOK, PPM, CtS and RM respectively) as a sequence of particles over time.

The total transmitted power for the four transmission is fix, $E_{seq} = 1^6$ particles, which corresponds to 100.000 particles per pulse in OOK, 50.000 particles per pulse in PPM, 333.000 particles per pulse in CtS and 33.333 particles per pulse in RM. According to the number of transmitted particles per pulse the range will be higher or smaller.

The time for the whole sequence is fix for any scheme: $T_{seq} = 0.03s$. The symbol time is fix for PPM and OOK and it is equal to $T_s = 0.003s$, for RM is equal to

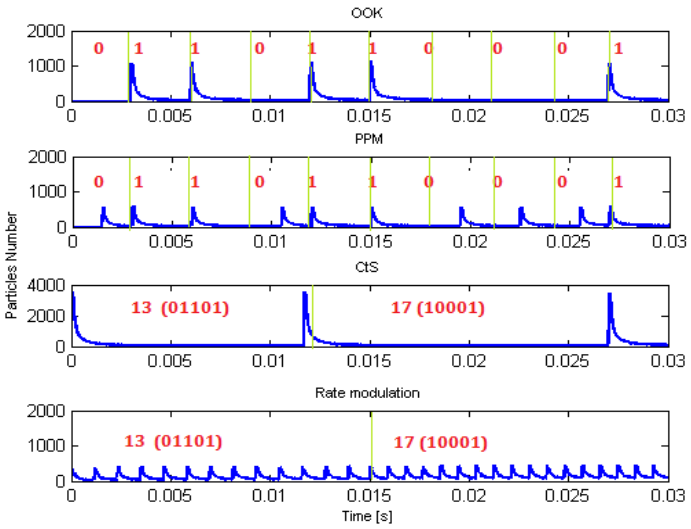

Figure 5.5: Reception process for OOK, PPM, CtS and RM for a distance of 500nm.

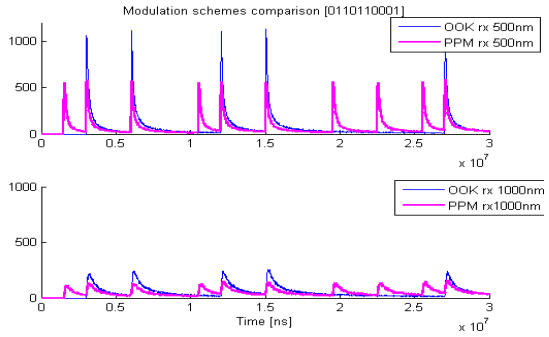

Figure 5.6: OOK Vs PPM received signal for a distance of 500nm (a) and 1000nm (b).

$T_s = 0.015s$ and it is variable for Cts scheme. The symbol time is chosen according to the data shown in table 5.1 as the time necessary for a receiver located at a distance of 1000nm to recover the information receiving at least 50% of the total received power.

Fig.5.5 shows the reception process for the four transmissions at a distance of 500nm. The vertical green lines show the symbol times for each modulation scheme and the red data the decoded information sequence the receiver recovers.

- In order to compare the performance of OOK to PPM fig.5.6 shows the reception of these two modulation schemes for two distances. The upper image is the number of particles measured by a receiver located 500nm away and the

-	1/after 0	1/after 1	mean value
OOK	14.9	10.46	9.65
PPM	6.04	8.65	7.89

Table 5.2: Peak to peak value for a distance of 1000nm

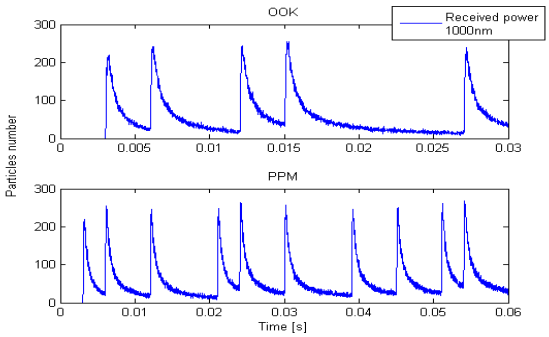

Figure 5.7: OOK (a) and PPM (b) received sequences for a distance of 1000nm.

lower image is the reception of a receiver located 1000nm away. As the T_s is fix, and it has been chosen to reach the distance 1000nm with a considerable SNR, the maximum rate is fix, $R = 333bps$. As we can see in the upper image the received signal owns a higher SNR, and a shorter T_s could be use in order to reach that distance with a better performance in terms of rate.

The transmission range is bigger for the OOK than for PPM, as the figure shows how the received OOK pulses present a higher peak value for both distances.

Table 5.2 shows the results of the $P - P$ value for a distance of 1000nm (higher the value better the performance) for different pairs of symbols (the worst cases). OOK outperforms PPM since OOK pulses are encoded using twice the energy per pulse used in PPM scheme, thus OOK pulses reach the receiver with a higher power compared to PPM pulses and they are easier to decode. Since in OOK one of the symbols is transmitted as a silence, the ISI is reduced.

- Furthermore, both modulations schemes (OOK and PPM) are analyzed by comparing the throughput. In this case, the E_s and T_s for both schemes are

-	E_s	T_s	R
OOK	$100.000[particles]$	$0.003s$	$333[bps]$
PPM	$200.000[particles]$	$0.015s$	$166[bps]$

Table 5.3: Energy per symbol, time per symbol, and throughput comparison table for distance 1000nm

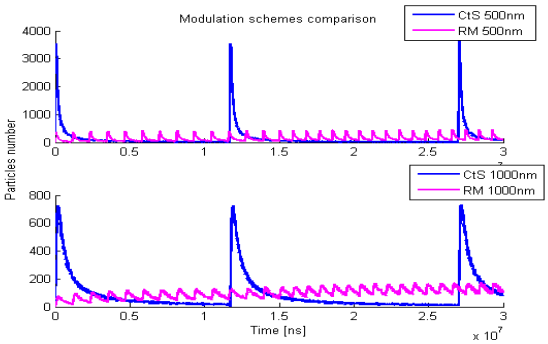

Figure 5.8: CtS Vs RM received signal for a distance of 500nm (a) and 1000nm (b).

adjusted in transmission to reach any distance with the same power per pulse. Fig. 5.7 upper image shows the received power for the OOK scheme and the lower image the received power for the PPM scheme, where we see the obtained ISI and amplitude of the pulses is equal. Table 5.3 shows the performance of both schemes by comparing the values of E_s, T_s and R, and we can see OOK outperforms PPM in throughput and energy management.

- In order to compare the performance of CtS to RM fig.5.8 shows the reception of these two modulation schemes for two distances. The upper image is the number of particles measured by a receiver located 500nm away and the lower image is the reception of a receiver located 1000nm away, for a T_{seq} and a E_{seq} fix in transmission. Table 5.4 shows the values of the peak to peak value.
  CtS outperforms RM as it was expected in term of ISI and transmission range. Furthermore, CtS, can be adjusted to reach a higher bandwidth by using a faster T_{clock}.

The results obtained by simulation point to PAM (OOK) as the most suitable modulation scheme to be used in the diffusion-based communication channel, in terms of simplicity (no overhead for synchronization), throughput, energy management,

-	'13'	'17'	mean value
Cts	–	–	76.37
RM	3.56	2.12	2.84

Table 5.4: Peak to peak value for a distance of 1000nm

and ISI.

In the literature, [28] proposes two modulation techniques for the diffusion-based communication channel: Concentration Shift Keying, CSK, and Molecule Shift keying, MSK. Both techniques are analyzed in a theoretical way by means of comparing the transmission power requirements and susceptibility to noise. The first one, CSK is similar to a 2-level PAM, in which a transmitter sends a '0' or a '1' according if it releases a n_o concentration level or a n_1. We improve this approached by proposing OOK, where a better management of the available power is used. The second one, MSK, is based on transmitting each symbol by transmitting a type of molecules. We have related this concept to diversity, it is is better used for creating several channels in an only communication scenario. (See Section 6.2).

Chapter 6

Noise Analysis and Interference Evaluation

6.1 Noise Analysis

6.1.1 Noise sources Overview

Brownian motion is a source of uncertainty in the space distribution of particles, and it causes the exact location of a particle to be unknown. As a consequence, even in a system with a homogeneous particle concentration, we cannot predict the exact number of particles within a space area.

When a receiver estimates the concentration by sensing the number of molecules within its actuation area over time, the uncertainty of Brownian motion is observed as a noise source, *i.e.*, an unwanted perturbation on the received concentration signal. We can observe this effect in Fig.6.3 that shows the concentrations estimated by three receives, and the signals present the mentioned fluctuations.

This effect has been modeled by means of a probabilistic model in [38], and it is called **Particle Counting Noise**, PCN. In this model, the number of particles Np measured by a receiver follows a non-homogeneous Poisson counting process, whose

rate of occurrence is equal to the actual concentration, $c(t)$:

$$N_p \sim Poiss(c(t))$$

This noise can be related to the shot noise in optical communications. Similarly to the shot noise, the Particle Counting Noise, is signal-dependent, *i.e.*, the higher is the power of the transmitted signal, the higher is the power of the noise that affects the received signal. The noise source of the particle counting noise is the diffusion process itself.

In the literature, we find two more noise sources present on the transmission over the diffusion-based channel.

The transmitted signal is discrete since it is composed by individual particles. The discretization of the signal in the emission process results on an unwanted perturbation on the transmitted concentration flux (or concentration rate), $r_T(t)$. The discretization of the signal in the emission process is identified as a noise source.

This effect has also been modeled by means of a probabilistic model in [38] and the name **Particle sampling noise**, PSN, has being assigned. The probabilistic study first models the outer concentration around the emitter with a double Non-Homogeneous Poisson Counting process. When the rate is positive, (transmitter releases particles), the process is positive and its rate of occurrence is the expected rate:

$$c_T(t) \sim Poiss(r(t)); (r > 0)$$

For a negative rate, (transmitter absorbs particles) the process is negative and its rate of occurrence of the poisson process is the negative rate:

$$c_T(t) \sim -Poiss(-r(t)); (r < 0)$$

From these results, the probabilistic model for the output concentration rate is defined as the time difference of a double non-homogeneous Poisson counting process with average value the expected rate. It is a white random process with its mean

squared value the particle concentration rate.
Finally, the third identified noise source is related to the reception process. The receiver estimates the concentration following the ligand-binding theory. This theory (explained in Section 2.2.2) models with non-linear kinetic equations how and when the ligand and the receptor become a complex. This noise is present as an unwanted perturbation on the internal decoded concentration in the receiver. In [39] expressions for the expected value and variance for this noise source are depicted.

6.1.2 Noise models validation results

We study through *N3Sim* the nature and the effect of the first two mentioned noise sources, known as **particle counting noise**, PCN, and **particle sampling noise**, PSN. *N3Sim* does not implements the ligand-binding theory in the reception process, thus, the third noise source can not be validated.

- We evaluate the PCN by simulating a bounded space containing a homogeneous concentration, and placing one-hundred receivers all over the space that measure the number of particles, N_p, over time. This scenario is repeated with different homogeneous concentration values. We check for each scenario (each concentration level) if the stochastic process that best model the obtained data set is the Poisson process with parameter equal to the actual concentration. The validation is done through the comparison of two likelihood tests.
  A likelihood test shows how likely a specific distribution is to follow a restricted one. In this case, our distribution is firstly compared to a Normal distribution with mean and variance equal to the actual concentration and it is secondly compared to a Poisson distribution with rate the actual concentration. The mean value of the likelihood tests are 0.91 and 0.9923, respectively. As a consequence, the simulation results indicate that diffusion-based noise is better modeled by the Particle Counting Noise from [38].

- We evaluate the PSN by simulating a transmission of particles, in an unbounded communication scenario without background concentration with a

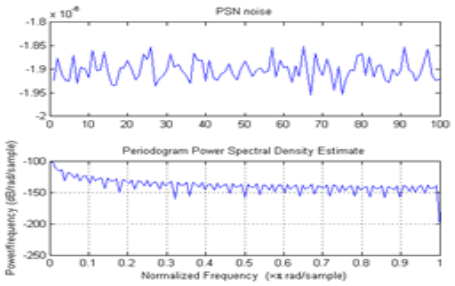

Figure 6.1: a) PSN b) Its power spectral density

concentration emitter that implies a concentration in its actuation space. We measure outgoing concentration with several receivers, located in the same place as the receiver, and we compare these measures with the expected flux of particles obtained by computing the net flux of particles should appear due to the concentration gradient, by using the first Fick's Law (Eq. 2.8). This noise appears as a perturbation in the outgoing flux. We verify that the its power spectral density is flat, and the power noise and the mean are equal to the expected rate. Fig.6.1 shows an example of the particle counting noise, and how its power spectral density is flat.

Both PSN and PCN are signal dependent noise sources.
Capacity in traditional EM channels is computed by following the Shannon formula, defined for memoryless channels, including channels impaired by additive white Gaussian noise (AWGN) for a given signal-to-noise ratio (SNR). The capacity for the diffusion-based channel model is a challenging parameter due to Shanon formula can not be directly applied, due to the non-additive noise sources.

6.2 Interferences Evaluation

In this section we study the interferences for the multi-transmitter scenario by distinguishing the two following cases:

1. When the multi-transmitter scenario behaves as a single channel, since each transmitter releases the same type of molecules into the medium.

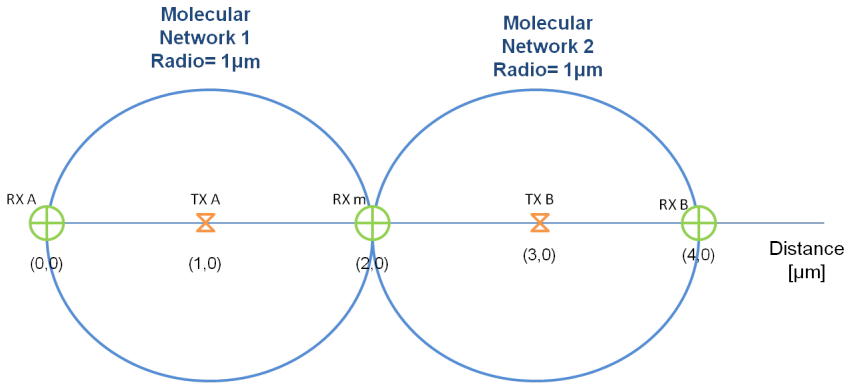

Figure 6.2: Multi-transmitter scenario for evaluation of interences between two nanocells.

2. When the multi-transmitter channel is treated as a composition of independent channels, since diversity is created due to each transmitter releases different kind of particles into the medium.

For the first case the results show that while interactions among diffusing particles have a negligible effect in the diffusion process, the channel is linear and the interferences affecting to any receiver depend on the distance between the receiver to each transmitter.

We evaluate the interferences in the communication scenario shown in Fig.6.2, where there are two transmitters, TXA and TXB, and three receivers, RXA, RXB, and RXM, located in the positions the figure shows. (All distances between a receiver and a transmitter are equal to $1\mu m$, and receiver and transmitters are all modeled with their transparent versions and with the same dimensions)

The communication scenario is divided into two 'nanocells', according to the envisioned transmission range for the diffusion-based communication alternative, in order to evaluate the interferences among adjacent 'nanocells' in a broadcasting communication scenario.

In the presented communication scenario, both transmitters, A and B, release particles to the medium following the same release pattern, a spike train. Fig 6.3 shows the concentration estimated by the three receivers. In the upper image, the concentration estimated by the receiver placed on the left side (RXA) is presented, in the second image the concentration estimated by the receiver placed in the middle

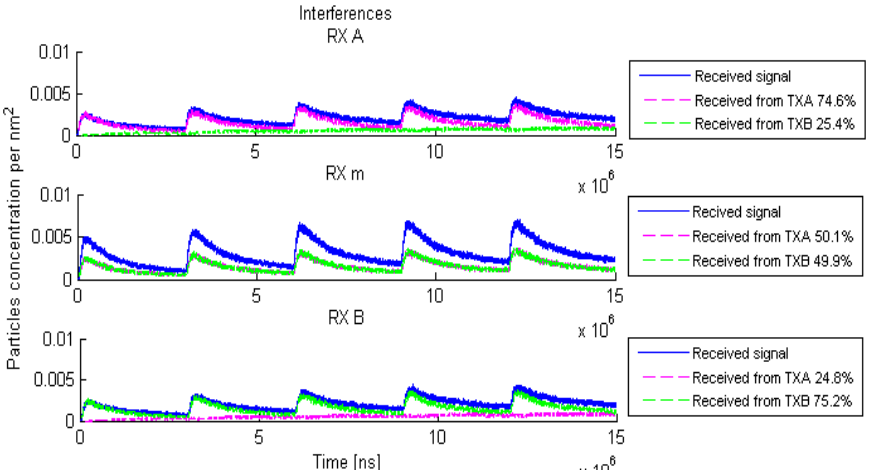

Figure 6.3: Estimated concentration by the three receivers, a) RXA, b) RXM and c) RXB respectively.

(RXM) is shown, and the lower image shows the corresponding concentration estimated by the receiver placed on the right side (RXB). Furthermore, each image shows the amount of received concentration coming from each transmitted. The evaluated metric is the noise-plus-interference ratio SINR, defined as:

$$SINR = \frac{P}{E[S^2] + E[W^2]} \tag{6.1}$$

where S is the interference signal, W the noise and P is the power of the received signal.

The total number of received particles is treated as signal power, the noise power is computed as the power of PCN, and the interference power is the total amount of particles coming from the transmitter which is outside the actual nanocell.

Table 6.1 shows the values of the SINR for the tree receptions. $SINR_{nanocellA}$value corresponds to the results of treating as signal the transmission of TXA and interference the power transmitted by the TXB, and the $SINR_{nanocellB}$ is performed by treating as signal the transmission of TXB and interference the power coming from TXA.

For the second case, when different emitters use different types of particles and

SINR	RXA	RXm	RXB
Nanocell A	3.96	1.98	1.32
Nanocell B	1.34	1.98	3.96

Table 6.1: Signal to noise plus interference ratio, evaluated in the three receivers

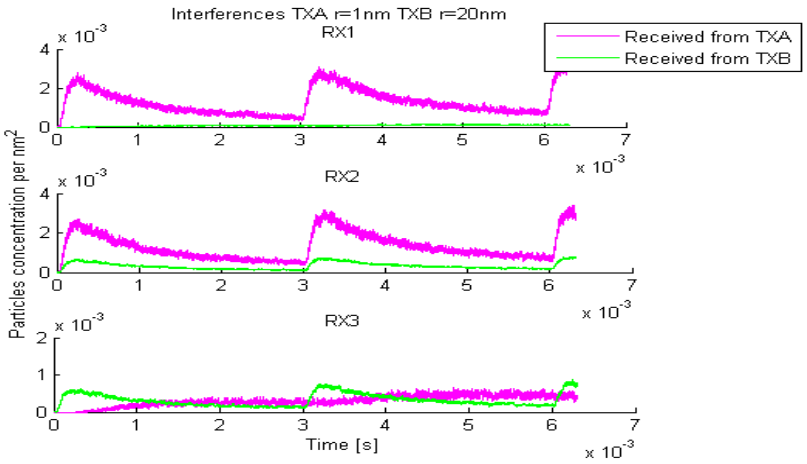

Figure 6.4: Multi-transmitter scenario for interences evaluation for different transmissions.

the interactions among them are negligible, independent channels are created and there is not interferences in the receiver. Capacity can be increased by using the *Molecular Division Multiple Access* technique proposed in [5].

Fig.6.4 shows the reception by the three receivers in the previous shown communication scenario (see Fig. 6.2) in case both transmitters use different types of molecules. TXA releases particles type A, e.g. calcium particles r=0.2nm , and transmitter TXB releases particles type B, e.g. potassium particles r=0.22nm. As the nature of the transmitted signals are different but the sizes are similar, the receiver is able to distinguish the concentration coming from transmitter A or from transmitter B and the multi-transmitter scenario behaves as a LTI channel, hence no interferences are present in the reception side.

However, when interactions affect to the transmission process, diversity concept cannot be applied, due to the channel is no longer linear, and the transmitted signal from TXA affect to the propagation of the transmitted signal from TXB.

As it is shown in previous sections, when the size of the transmitted particles is

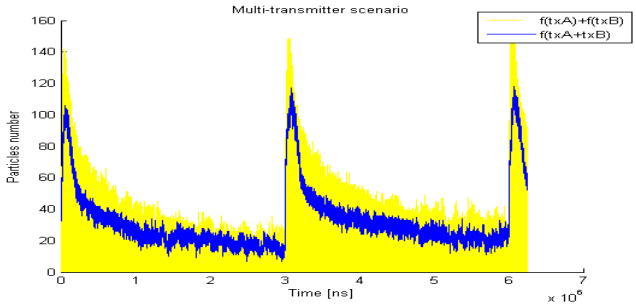

Figure 6.5: Multi-transmitter scenario no linear behavior.

increased the effect of interactions is no longer negligible.

We test if the previous scenario, 2-transmitter scenario (see 6.2) is linear for a transmission of particles with radius=20nm. Both transmitters, A and B, (TXA, TXB) release the same sequence of particles, TXA releases particles of size r=20nm and TXB releases particles of size r=22nm.

Fig. 6.5 shows in blue the reception when both transmitter releases the signal at the same time, and in yellow the sum of both receptions in case they were independent transmissions. The yellow colored are does not match with the blue curve, thus, the channel is no linear for the tested scenario due to the linearity property is not fulfilled.

Chapter 7

Conclusions and future work

7.1 Conclusions

Nanonetworking or the association of nanomachines, is expected to expand the capabilities and operation range of nanomachines, by providing them a way of sharing information. When the concept of nanonetworking came up, the usage of EM waves was disregarded as a communication alternative, due to the fact EM waves did not scale to nano-sizes; as a result, the first concepts of MC emerged. After that, carbon materials were proposed and they opened the door to the use of EM waves in the nano-scale. The goal today is to assess how nano-machines will best communicate. What seems clear is that for intra-body nanonetworks, MC is the best approach, but the channel capacity available for the different proposed techniques is still unclear. With this simulation-based exploration of the diffusion-based communication channel we have provided communication metrics and insight into the physical layer of this communication paradigm.

Summary of contributions

- The LTI property is proven to be a valid assumption for normal diffusion-based MC single/multi-transmitter scenarios. We have shown how the channel is well modeled under Fick's laws when interactions among the diffusing particles do not change the diffusion process, or the fluid characteristics, since they model

a diffusing scenario where particles totally ignore what the other particles from the considered concentration are doing.

- Interactions among diffusing particles can change the diffusion process, specially when the considered concentration is high. When the final process differs from normal diffusion is known as anomalous diffusion and Fick's diffusion law fails in modeling the distribution of particles.
  We have proven that when the nature of interactions among diffusing particles differs from the interactions between diffusing particles and those form the fluid, the effect of those interaction can not longer be neglected (such as elastic collisions where more kinetic energy is exchanged). Furthermore, when the fluid nature allows to add inertia to the displacement defined by the Brownian dynamics (which depends on the Reynolds number), the final process underling the anomalous diffusion is the correlated random walk.
  For the general case of anomalous diffusion, we conclude the LTI property is a valid assumption for the single-transmitter scenario but no for the multi-transmitter scenario.

- We provide results for the channel transfer function of the normal diffusion-based channel, by representing the attenuation and the group delay with respect to the frequency and the transmission range. The results show the channel behaves as a low pass filter only allowing slow signals to propagate. The bandwidth of the channel resides mainly on the diffusion coefficient, which results in a faster or a slower diffusion process.

- We have provided guidelines for molecular signaling. We show how the power is best distributed in order to reach a distance with the highest SNR and lower ISI; and how the total transmitted power determines the received power, regardless the pulse shape in which the particles have been transmitted.
  The operation range of nanomachines is limited by the total number of emitted particles. Since we have observed that the normal diffusion-based channel is LTI, the effect of one transmitter releasing a certain number of particles to the

medium is equivalent to two transmitters, each releasing half of this quantity. Therefore, by adding emitters that transmit coordinately we can extend the range of the transmitted signal.

Furthermore, we have determined that the shorter the pulse in transmission, the wider the bandwidth in reception. The distortion (shape widening) any signal suffers when passing through the channel, is the most important parameter limiting the bandwidth.

- We find that the diffusion-based molecular channel is an appropriate technique to broadcast information when the transmitter and the receiver are in close proximity in space. A high degradation of the expected capacity for this channel appears when the distance increases, as the mean delay increases with the square of the distance.

- We have determined that OOK modulation scheme based on a spike pulse as its basis, outperforms the other tested modulation techniques in simplicity, transmission range, noise, ISI, and bit rate. The obtained results show that a trade off exists between ISI and bandwidth. Our results point out that in a molecular nanonetwork, in order to minimize the overall energy consumption while allowing for a correct reception of the transmitted signal, the transmitter nanomachines should be able to adjust the energy and the duration of the transmitter pulses.

- Diffusion-based noise (known as Particle Counting Noise) is observed and evaluated with reference to already proposed stochastic models, and the discretization of the signal in transmission is observed as a noise source present in the outgoing flux of particles.

- Finally, we have shown how interferences can degrade or improve the communication process when different transmitters release the same or different type of molecules, respectively.

7.2 Future Work

Nanonetworking is a multidisciplinary field of research that is attracting more and more the interest of researchers from different domains, and in which, in order to move forward, people from those domains should share their knowledge.

Future work on this field should continue with the development of an information theory to reach the channel capacity, in which, the channel modeling, the noise features, and encoding and decoding techniques were tailored to the channel singularities, and the results should be contrasted with a simulation tool.

Further research of this communication paradigm should cover aspects regarding network architecture and communication protocols such as: channel sharing, addressing, information routing and reliability issues.

We have presented in this work *N3Sim*, we have shown its benefits respect to other diffusion-based molecular communication simulators, which result from the fact that it simulates the motion of every single molecule independently, which allows for the observation of the effect of the molecule interactions and the uncertainty introduced by the Brownian motion. The extension of *N3Sim* to model the reception process following the ligand-binding theory, would result in the obtainment of more realistic results for the entire communication process. Furthermore the third proposed noise source *Reception noise* [39] could be explored. The scalability of *N3Sim* to simulate more complex scenarios, thus more realistic nanonetworks, must be improved.

N3Sim could also be extended to to provide a simulation framework for all techniques proposed within MC, such as the propagation of bacteria, molecular motors, and a flow-based diffusion scenario.

Bibliography

[1] Cambridge university science magazine.

[2] Ian F. Akyildiz, Fernando Brunetti, and Cristina Blàzquez. Nanonetworks: A new communication paradigm. *Computer Networks*, 52:2260 – 2279, 2008.

[3] Ian F Akyildiz and Josep Miquel Jornet. Electromagnetic wireless nanosensor networks. *Computer Networks*, 2010.

[4] Ian F. Akyildiz and Josep Miquel Jornet. The internet of nano-things. *Wireless Commun.*, 17:58–63, December 2010.

[5] Ian F. Akyildiz and Parcerisa Lluis. Molecular Communication Options for Long Range Nanonetworks. *Computer Networks*, 53(16):2753–2766, 2009.

[6] Baris Atakan and B. Ozgur Akan. Deterministic capacity of information flow in molecular nanonetworks. *NanoCommunication Networks*, 2010.

[7] Baris Atakan and Ozgur B Akan. Single and Multiple-Access Channel Capacity in Molecular Nanonetworks. *Middle East*.

[8] Baris Atakan and Ozgur B Akan. On Channel Capacity and Error Compensation in Molecular Communication. *Springer Transactions on Computational Systems Biology*, 10:59–80, 2008.

[9] Baris Atakan and Ozgur B Akan. Carbon nanotube sensor networks. *Energy*, pages 1–6, 2009.

[10] Sarika Bhattacharyya and Biman Bagchi. Anomalous diffusion of small particles in dense liquids. *Chem. Phys*, 106:1757–1763, 1997.

[11] P D Bons and B A Carreras. On the applicability of Ficks law to diffusion in inhomogeneous systems. 26:913–925, 2005.

[12] H.a. Botero Castro and J.M. Ramirez Scarpetta. A Methodology For Excitation Systems Identification. *2005 International Conference on Industrial Electronics and Control Applications*, pages 1–6.

[13] Naama Brenner, Oded Agam, William Bialek, and Rob de Ruyter van Steveninck. Universal Statistical Behavior of Neural Spike Trains. *Physical Review Letters*, 81(18):4000–4003, November 1998.

[14] D L Ermak and J A Mccammon. Brownian dynamics with hydrodynamic interactions. *J. Chem. Phys.*, 69:1352–1360, 1978.

[15] Robert A Freitas. Nanotechnology, nanomedicine and nanosurgery. *International Journal of Surgery*, 3(4):243–6, January 2005.

[16] Wulfram Gerstner, Andreas K. Kreiter, Henry Markram, and Andreas V. M. Herz. Neural codes: Firing rates andbeyond. *Proceedings of the National Academy of Sciences of the United States of America*, 94(24):12740–12741, November 1997.

[17] Maria Gregori and Ian F. Akyildiz. A new nanonetwork architecture using flagellated bacteria and catalytic nanomotors. *IEEE J.Sel. A. Commun.*, 28(4):612–619, 2010.

[18] Maria Gregori, Ignacio Llatser, Albert Cabellos-Aparicio, and Eduard Alarcn. Physical channel characterization for medium-range nanonetworks using catalytic nanomotors. *Nano Communication Networks*, 1(2):102 – 107, 2010.

[19] Maria Gregori, Ignacio Llatser, Albert Cabellos-Aparicio, and Eduard Alarcn. Physical channel characterization for medium-range nanonetworks using flagellated bacteria. *Computer Networks*, 55(3):779 – 791, 2011.

[20] Ertan Gul, Baris Atakan, and Ozgur B. Akan. Nanons: A nanoscale network simulator framework for molecular communications. *Nano Communication Networks*, 1(2):138 – 156, 2010.

[21] John E. Hall. *Guyton and Hall Textbook of Medical Physiology*. Mosby, eleventh edition edition, 2007.

[22] M. Pierobon I. Llatser, E. Alarcn. Diffusion-based channel characterization in molecular nanonetworks. *IEEE MoNaCom 2011*, 2011.

[23] S.W Jakobsson, E.; Chiu. Application of brownian motion theory to the analysis of membrane channel ionic trajectories calculated by molecular dynamics. *Biophysical journal*, pages 751 – 756.

[24] Josep Miquel Jornet and Ian F Akyildiz. Graphene-Based Nano-Antennas for Electromagnetic Nanocommunications in the Terahertz Band. *European Conference on Antennas and Propagations*, 2010, Barcelona.

[25] R. Kadloor, S. Adve. A framework to study the molecular communication system. *Computer Communications and Networks, 2009. ICCCN 2009. Proceedings of 18th Internatonal Conference on*, 2009.

[26] Sachin Kadloor, Raviraj S. Adve, and Andrew W. Eckford. Molecular communication using brownian motion with drift. *CoRR*, pages –1–1, 2010.

[27] Hendrik A Kooijman. A Modification of the Stokes-Einstein Equation for Diffusivities in Dilute Binary Mixtures. *Ind. Eng. Chem*, 41:3326–3328, 2002.

[28] H. B. Tugcua T. Akyildiz I. F. Kuran, M.S. Yilmaz. Modulation techniques for communication via diffusion in nanonetworks.

[29] H. B. Tugcua zermanb B. Kuran, M.S. Yilmaz. Energy model for communication via diffusion in nanonetworks. 2010.

[30] Kwan S. Kwok and James C. Ellenbogen. Moletronics: future electronics. *Materials Today*, 5(2):28 – 37, 2002.

[31] Liu J. Q. Nakano T. Liu, J. Q. and T. Nakano. An information theoretic model of molecular communication based on cellular signaling. *1st International ICST Workshop on Computing and Communications from Biological Systems: Theory and Applications*, May 2007.

[32] Fedotov S Horsthemke W Mndez, V. *Reaction-Transport Systems: Mesoscopic Foundations, Fronts, and Spatial Instabilities*. Springer, 2010.

[33] Michael Moore, Akihiro Enomoto, Tadashi Nakano, Ryota Egashira, Tatsuya Suda, Atsushi Kayasuga, Hiroaki Kojima, Hitoshi Sakakibara, and Kazuhiro Oiwa. A Design of a Molecular Communication System for Nanomachines Using Molecular Motors. *Network*, 2006.

[34] T Nakano, T Suda, M Moore, R Egashira, A Enomoto, and K Arima. Molecular communication for nanomachines using intercellular calcium signaling. *Fifth IEEE Conference on Nanotechnology*, 2:478–481.

[35] David L. Nelson and Michael M. Cox. *Lehninger Principles of Biochemistry, Fourth Edition, Chaper 12, Biosignaling*. W. H. Freeman, fourth edition edition, April 2004.

[36] Oxon O X Oqx. Application of System Identification techniques to an RF cavity tuning Loop. *Time*, (2):982–984.

[37] Jean Philibert. One and a Half Century of Diffusion : Fick , Einstein , Before and Beyond. *Materials Science*, 4:1–19, 2006.

[38] M. Pierobon and I. F. Akyildiz. Diffusion-based Noise Analysis for Molecular Communication in Nanonetworks. *to appear in IEEE Transactions on Signal Processing, 2011.*

[39] M Pierobon and I F Akyildiz. Reception Noise Analysis for Molecular Communication in Nanonetworks.

[40] M Pierobon and I F Akyildiz. A physical End to End Model for Molecular Communication in Nanonetworks. *Journal of Selected Areas in Communications (JSAC)*, 2010.

[41] M. Pierobon and I. F. Akyildiz. Information capacity of diffusion-based molecular communication in nanonetworks. *Proc. IEEE Infocom Miniconference*, 2011.

[42] R. Pintelon and J. Schoukens. *System identification: a frequency domain approach*. 2001.

[43] Gabriel A. Silva. Introduction to nanotechnology and its applications to medicine. *Surgical Neurology*, 61:216 – 220, 2004.

[44] Tatsuya Suda, Michael Moore, Tadashi Nakano, Ryota Egashira, and Akihiro Enomoto. Exploratory Research on Molecular Communication between Nanomachines. *Natural Computing*, 2005.

[45] S Sung. Pseudo-random binary sequence design for finite impulse response identification. *Control Engineering Practice*, 11(8):935–947, August 2003.

[46] Raúl Toral. *Últimos avances en el movimiento Browniano: orden a partir del desorden'*. Cátedra de divulgacin de la ciencia de la universidad de valencia csic edition.

[47] Loukas Vlahos, Heinz Isliker, Yannis Kominis, and Kyriakos Hizanidis. Normal and Anomalous Diffusion: A Tutorial, May 2008.

[48] Dehui Wang and C D Johnson. Identification Methods. *Computer Engineering*, 000:52–56, 1989.

[49] Moe Z Win, Senior Member, and Robert A Scholtz. Impulse Radio : How it works. *Communications*, 2(1):10–12, 1998.

[50] Yujie Zhu and Raghupathy Sivakumar. Challenges : Communication through Silence in Wireless. *Computer Engineering*, 2005.

Simulation-based Evaluation of the Diffusion-based Physical Channel in Molecular Nanonetworks

Nora Garralda*, **Ignacio Llatser***, **Albert Cabellos-Aparicio***, **Eduard Alarcón***, **Massimiliano Pierobon**†

*NaNoNetworking Center in Catalunya (N3Cat)
Universitat Politècnica de Catalunya
Barcelona, Spain
E-mail: {garralda, llatser, acabello}@ac.upc.edu, ealarcon@eel.upc.edu

† Broadband Wireless Networking Laboratory
School of Electrical and Computer Engineering
Georgia Institute of Technology, Atlanta, Georgia 30332, USA
E-mail: maxp@gatech.edu

***Abstract*—Nanonetworking is an emerging field of research, where nanotechnology and communication engineering are applied on a common ground. Molecular Communication (MC) is a bio-inspired paradigm, where Nanonetworks, i.e., the interconnection of devices at the nanoscale, are based on the exchange of molecules. Amongst others, diffusion-based MC is expected to be suitable for covering short distances (nm-μm). In this work, we explore the main characteristics of diffusion-based MC through the use of *NanoSim*, a physical simulation framework for MC. *NanoSim* allows for the simulation of the physics underlying the diffusion of molecules for different scenarios. Through the *NanoSim* results, the Linear Time Invariant (LTI) property is proven to be a valid assumption for the free diffusion-based MC scenario. Moreover, diffusion-based noise is observed and evaluated with reference to already proposed stochastic models. The optimal pulse shape for diffusion-based MC is provided as a result of simulations. Two different pulse-based coding techniques are also compared through *NanoSim* in terms of available bandwidth and energy consumption for communication.**

I. Introduction

Nanomachines are the simplest devices in the nanoscale, able to perform tasks such as computing, sensing, information storage and actuation. Nanonetworks, i.e., the interconnection of nanomachines, allow cooperation among them in order to fulfill more complex tasks and increase their operation range, thus expanding their capabilities. Nanonetworks are expected to be applied in many different fields, ranging from the environmental, to the industrial and the biomedical [1].

Amongst other proposed techniques, molecular communication enables the interconnection of nanomachines through the exchange of molecules. Molecular communication spans several different communication solutions according to the way molecules are propagated and they are classified in relation to the communication range. For short distances (nm-μm), molecular motors [2] and calcium signaling have been proposed [3], [4]; for the medium range (μm-mm), the use of the flagellated bacteria and catalytic nanomotors [5] has been studied and simulated; for the long range (mm-m), communication by means of pheromones has been suggested [6] as a possible solution.

This work is focused on diffusion-based molecular communication, where information is encoded by the transmitter nanomachine in the molecule release pattern, creating a specific sequence of molecules concentration values at the transmitter location. These changes in the concentration eventually reach a receiver nanomachine, which is placed at a distance from the transmitter. The propagation of the changes in the molecule concentration is due to the diffusion process. The receiver decodes the transmitted information by sensing the local concentration at its location [7].

Diffusion-based molecular communication, and the resulting molecular nanonetworks, are especially aimed to intra-body scenarios due to their low power requirements and high biocompatibility. Potential applications of molecular nanonetworks include, but are not limited to, intelligent drug delivery systems, diagnostic and therapeutic antiviral activities, and prosthetic implants techniques [8], [9], [10].

Several research efforts have been focused on the physical modeling of the channel in diffusion-based molecular communication. As an example, physical models for the channel as well as bio-inspired transmitters and receivers are provided in [7]. Information-theoretical approaches which compute the channel capacity have also been applied in [11], [12], [13], [14]. We believe that in order to validate these models and provide a common ground to compare them, tests either by means of simulation or experimentation should be provided.

The work presented in this paper is focused on the study of the diffusion-based molecular communication channel by using the simulation framework *NanoSim*. Through *NanoSim* we are able to simulate the physics underlying the propagation of molecules in different molecular communication scenarios. As a result, we obtain several parameters related to the communication characteristics of the diffusion-based molecular communication channel, such as the attenuation, the delay and the noise features. *NanoSim* enables also the comparison between different modulation schemes for the diffusion-based molecular communication.

The remainder of this paper is organized as follows. In Section II, we introduce the physical layer simulator for the diffusion-based molecular channel, *NanoSim*. In Section III, we review the different diffusion scenarios related to the assumptions on the physical behavior of the molecules. In Section IV, we examine the noise in a molecular channel and we validate it by simulation. In Section V, we prove that the diffusion-based molecular communication channel is linear and time-invariant. In Section VI, we show the effects of changing the shape and length of the transmitted pulses. Next, in Section VII, we evaluate several modulation techniques and we find the optimal scheme in terms of communication performance. Finally, Section VIII concludes the paper.

II. NanoSim Overview

NanoSim is a simulation framework for the general case of diffusion-based molecular communication, which simulates the diffusion-based molecular channel according to the Brownian dynamics of the molecules in a fluid medium. Through *NanoSim*, we also simulate interactions among the molecules, such as elastic collisions, when molecules exchange kinetic energy, or electrostatic interactions that appear when the molecules have an electrical charge. As an extension of the Brownian motion, *NanoSim* simulates also the correlated random walk.

The user can edit multiple parameters, such as the number of transmitters/receivers (as well as their locations), the radius of emitted molecules, the emission pattern for each transmitter, the fluid viscosity and the diffusion coefficient, and a bounded/unbounded space, amongst others.

Through *NanoSim*, a user may choose how the transmitter encodes the information: i) into the number of emitted molecules, known as information molecules, or ii) into the molecule concentration at the transmitter location. Furthermore, receivers estimate the local concentration by counting the number of molecules within their sensing area over time. The user may also choose between two types of receiver: i) an ideal receiver transparent to the diffusion process, and ii) a receiver that absorbs the molecules after they enter its actuation area.

The benefits of *NanoSim* with respect to other diffusion-based molecular communication simulators, [15] and [16], comes from the fact that it simulates the motion of every single molecule independently, which allows for the observation of the effect of the molecules interactions and the uncertainty introduced by the Brownian motion. Moreover, *NanoSim* allows the simulation of scenarios having virtually any number of transmitters and receivers. This feature enables simulations where the molecular information is broadcast from one transmitter to many receivers, or where more than one transmitter access the channel at the same time.

III. Molecular Diffusion Simulation scenarios

The diffusion process is defined as the spontaneous spread of molecules in the space upon a molecule concentration gradient. This process tends towards the homogenization of the molecule concentration in the fluid medium, causing a net flux of molecules from zones with higher concentration to the lower concentration zones [17].

The diffusion process is mathematically modeled by the Fick's laws of diffusion for the case of having a moderate concentration of molecules, so that each molecule motion can be considered as independent [18]. Brownian motion is the continuous-time stochastic process which underlies diffusion, and it is observed in a microscopic scale as the jittery motion that the molecules show upon collision with other neighboring molecules.

Brownian dynamics defines the mean square displacement of a molecule subject to diffusion, in each direction, as $\langle x \rangle^2 = 2Dt^{\alpha}$. D is the diffusion coefficient, defined for spherical molecules whose mass and size are much larger than those of the medium in which they are floating. This case corresponds to low Reynolds number conditions [19], which means that viscous forces dominate the process. When the mean square displacement is directly proportional to time, $\alpha = 1$, then the resulting process is called free diffusion. This scenario, can be simulated through *NanoSim*, which models the motion of every single molecule following the Brownian dynamics, and the results are validated by comparison to the Fick's laws of diffusion.

When $\alpha < 1$ or $\alpha > 1$, the resulting process is called anomalous diffusion. Collective diffusion is a case of anomalous diffusion and it occurs when there is a very high concentration of molecules. Due to the large amount of molecules, the interactions between them impact the diffusion process, which can no longer be modeled with the Fick's laws of diffusion.

The mathematical process underlying anomalous diffusion is the correlated random walk, a Lèvy process [20] which includes memory. This contrasts with the Brownian motion, whose main feature is the absence of time correlation, thus being a memoryless process. Correlated random walk is a discrete version of the Brownian motion, that spans the whole range of random walks, from ballistic to dispersal motions [21], where molecules always experience the same step size and they change their direction with a certain probability. The macroscopic view of the correlated random walk is modeled by the hyperbolic diffusion equation.

NanoSim allows modeling collective diffusion by simulating a large number of molecules and by taking into account elastic collisions among them. The observed results are that, in the tested scenarios, collisions among the information molecules have the same effect as collisions among the information and the fluid molecules. As a result, in this scenario the Fick's laws are a valid model for the molecule diffusion. Nevertheless, if electrostatic interactions are taken into account, these forces dominate the particle motion, which is then much faster and more directed than in the free diffusion and the Fick's laws are not longer valid. Finally, by adding an initial velocity to the emitted molecules, as well as inertia, which is the property of a molecule to remain at a constant velocity, *NanoSim* approximates the case of correlated random walk. The results for this case are validated by comparison to the hyperbolic

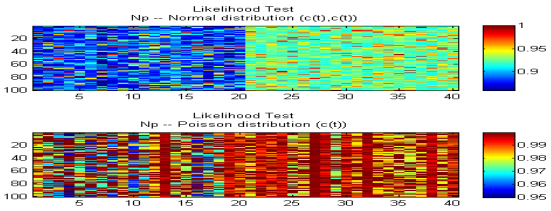

Fig. 1. Normal and Poisson Likelihood tests comparison

diffusion equation solution [7].

All the simulations performed throughout this paper consider the free diffusion scenario, and the space is considered as 2-dimensional.

IV. Noise in Diffusion-based Molecular Communication

Brownian motion is a source of uncertainty in the space distribution of particles, and it causes the exact location of a particle to be unknown. As a consequence, even in a system with a homogeneous particle concentration, we cannot predict the exact number of particles within a space area.

When a receiver estimates the concentration by sensing the number of molecules within its actuation area over time, the uncertainty of Brownian motion is observed as a noise source, i.e., an unwanted perturbation on the received concentration signal. This effect has been modeled by means of a probabilistic model in [22], and it is called Particle Counting Noise. In this model, the number of particles Np measured by a receiver follows a non-homogeneous Poisson counting process, whose rate of occurrence is equal to the concentration $c(t)$ of molecules: $N_p \sim Poiss(c(t))$

We have validated the diffusion noise through *NanoSim* by verifying that the number of particles in a space follows a non-homogeneous Poisson counting process, with the actual concentration as the rate of the process, by the comparison of two likelihood tests.

We consider a scenario with two different homogeneous concentrations of molecules over time. We first simulate the system with the lower concentration and after that we apply the higher one. We have created our data set by locating one hundred receivers all over the system that estimate the concentration independently. Each estimation shows unique values with respect to other estimation performed by other receivers in the same conditions. This is a consequence of the Particle Counting Noise.

In Fig. 1, we can see the result of two likelihood tests. The upper likelihood test shows how likely the number of measured molecules Np is to follow a normal process with mean and variance equal to the actual concentration. The lower likelihood test shows how likely is Np to follow a Poisson process with rate equal to the actual concentration. The mean value of the likelihood tests are 0.91 and 0.9923, respectively. As a consequence, the simulation results indicate that diffusion-based noise is better modeled by the Particle Counting Noise from [22].

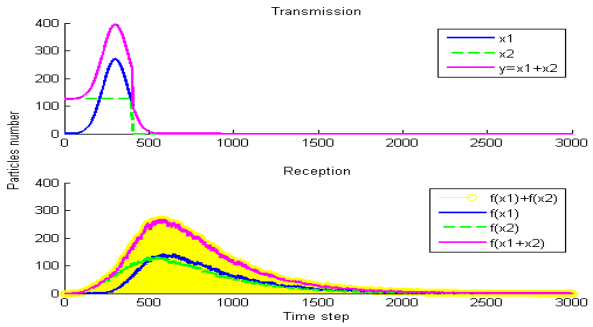

Fig. 2. Linearity validation for the single user scenario by verifying the homogeneity and additive properties. Transmission and reception of a Gaussian pulse, a square pulse and the addition of both.

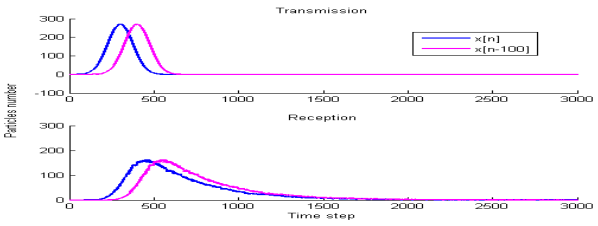

Fig. 3. Temporal invariance validation for the single-transmitter scenario. Transmission and reception of two Gaussian pulses in different times.

This noise can be related to the shot noise in optical communications. Similarly to the shot noise, the Particle Counting Noise, is signal-dependent, i.e., the higher is the power of the transmitted signal, the higher is the power of the noise that affects the received signal.

V. Channel Linearity and Time Invariance

A Linear Time-Invariant (LTI) channel fulfills the superposition principle, as well as maintains its features over time. In order to verify whether the molecular diffusion-based channel has the LTI property, we have considered two cases: the *single-transmitter scenario* and the *multi-transmitter scenario*. We analyze them in the following:

A. Single-transmitter scenario

In Fig. 2, the superposition principle is verified. The upper image shows three different transmitted signals: a Gaussian pulse ($x1$), a square pulse ($x2$), and the addition of both pulses ($y = x1 + x2$). The lower image shows the reception of these pulses at a certain distance, as well as the colored area which is the sum of the outputs as if their corresponding inputs where applied independently with respect to the channels. As it is shown in Fig. 2, the colored area matches with the output of the sum of the transmitted signals. These results should confirm the linearity of the channel.

The upper image of Fig. 3 shows the transmitted signals, two Gaussian pulses, one delayed with respect to the other, ($x[n]$, $x[n-100]$). The lower image of Fig. 3 shows the reception of the pulses, and how the delay between the outputs

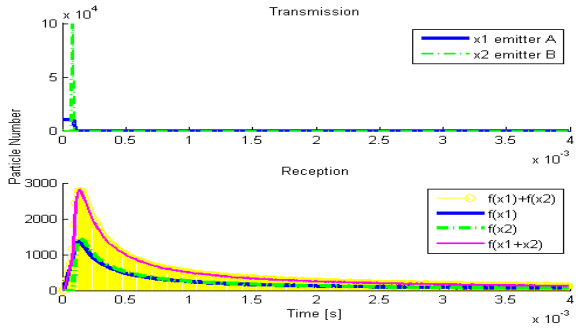

Fig. 4. Linearity validation for the multi-user scenario by verifying the homogeneity and additive properties. Transmission and reception of two square pulses, one wider than the other but with the same transmitted energy.

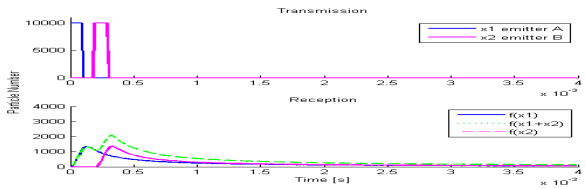

Fig. 5. Temporal invariance validation for the multi-user scenario. Transmission and reception of two square pulses from different emitters, in different times.

matches with the delay between the corresponding inputs. As a consequence, the channel behaves as time-invariant.

B. Multi-transmitter scenario

For the case of having more than one transmitter, first, transmitter A transmits a pulse, and after that, a second transmitter B transmits another pulse. When both pulses are transmitted at the same time, we check whether an equidistant receiver measures the same signal power as the sum of the two outputs corresponding to single pulses transmitted independently

In Fig. 4, the superposition principle is validated. We observe in the upper image the transmission of two different signals from transmitters A and B, a square pulse ($x1$), and a spike of particles ($x2$) as the narrowest possible pulse emitted, both containing the same energy. The lower image shows the reception by a receiver 500 nm away from both transmitters, ($f(x1)$,$f(x2)$), as well as the reception of the simultaneous transmission of the two pulses ($f(x1 + x2)$). Finally, the colored area shows the sum of the two independent transmissions ($f(x1) + f(x2)$). This area matches with the received signal corresponding to the emission of both pulses simultaneously, thus confirming that the channel shows the linearity property also for the multi-transmitter case.

In Fig. 5, we observe that the channel is time-invariant also for the multi-transmitter case. The upper image shows both transmitters, A and B, transmitting a square pulse in different time instants, ($x1$, $x2$). The lower image shows the reception of each transmission, ($f(x1)$, $f(x2)$) at a distance of 500 nm from the transmitters, and the received signal when both transmitters are transmitting simultaneously ($f(x1 + x2)$). Again, we conclude that the delay among the transmitted pulses is the same whether or not they are transmitted simultaneously.

In conclusion, we have obtained that the channel satisfies both conditions of linearity and time invariance for both scenarios, the single-transmitter scenario and the multi-transmitter scenario. This means that when different transmitters transmit the same type of particles, the interactions among them are negligible and the channel can be modeled through the Fick's laws of diffusion.

The operation range of nanomachines is limited by the energy of the transmitted pulses or, equivalently, the total number of emitted particles. Since we have observed that the channel is LTI, the effect of one transmitter releasing a certain number of particles to the medium is equivalent to two transmitters, each releasing half of this quantity. Therefore, by adding emitters that transmit coordinately we can extend the range of the transmitted signal.

If different emitters use different types of particles and the interactions among them are negligible, the channel capacity can also be increased by creating independent channels, e.g., by using the *Molecular Division Multiple Access* technique proposed in [6].

VI. Pulse Shaping

Due to their simplicity, the communication techniques based on the exchange of concentration pulses seem to be the most reasonable for diffusion-based molecular communication. In the following, we simulate the transmission of different pulse shapes in order to find the optimal shape for pulse-based modulations.

As Fig. 2, 3, 4 and 5 show, the transmitted pulse shape is distorted due to the diffusion process. For any possible transmitted pulse shape, the receiver gets a pulse with a long tail that follows an exponential decay. The widening in reception of the transmitted pulses increases with the distance, and limits the maximum achievable bandwidth.

With the objective of testing the channel behavior for different input pulse shapes, we compare three different shapes: a square pulse, a cosine pulse, and a Gaussian pulse. We consider these shapes due to their differences in the frequency domain; for the same time duration, the Gaussian pulse has its frequency components concentrated around the low frequencies, the square pulse is the more widespread in frequency and the cosine pulse is in between.

We evaluate the suitability of each of these pulses by comparing the widening and the attenuation of the received signal for some distance values. The time duration and total energy of the transmitted pulses are fixed to a common value for all three pulse shapes.

Fig. 6 shows the transmission and reception of the three pulses, for a range of 400 nm. The green vertical lines correspond to the time instants when the received signal has the 50%, 60%, 70%, 80% and 90% of the total received energy, from left to right, respectively. We observe that all the received pulses have a long tail and they are therefore distorted, albeit with a different degree of distortion. The

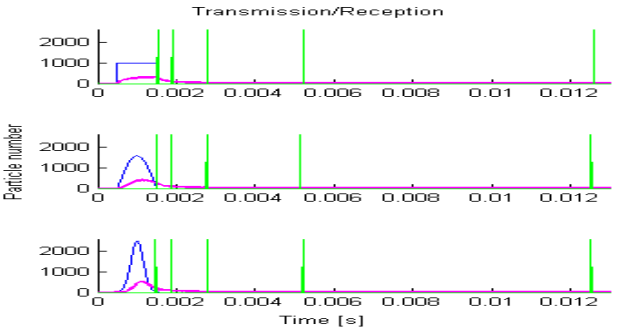

Fig. 6. Square, cosine and Gaussian pulses transmission and its reception by a receiver located 400 nm away.

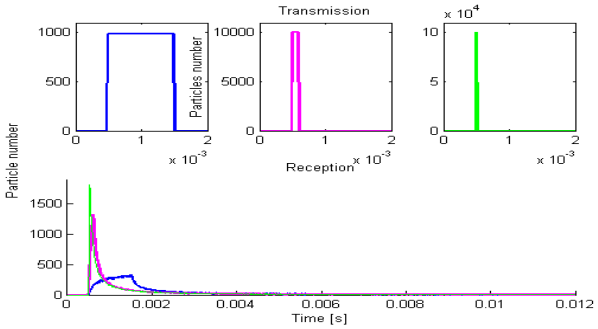

Fig. 7. Transmission and reception of square pulses with the same energy and different time durations.

Gaussian pulse (in the third image) shows the least amount of distortion, while the square one (in the first image) is the most distorted one. The maximum peak level in reception is obtained for the Gaussian pulse. The vertical lines in Fig. 6 show that the energy distribution of the received pulses has almost no dependence on the pulse shape. In conclusion, for a pulse transmission constrained in its energy and in the time duration, the Gaussian shape yields to the best performance, even though the differences with other shapes are minimal.

The widening in the received pulse is distance-dependent. This width determines the maximum achievable bandwidth for this distance. A decrease in the width of the received pulse, and therefore an increase in the achievable bandwidth, can be achieved by transmitting shorter pulses in time. Fig. 7 shows this effect. In the upper side of Fig. 7, the transmitted square pulses are shown, all of them with the same energy but having different lengths. The lower image shows the received pulses for the three transmissions; we observe that the minimum width corresponds to the case of transmitting the shortest square pulse.

After this analysis, we conclude that: i) the optimal pulse shape is a spike, a very narrow pulse, which gives the lowest pulse width at the receiver and thus the highest achievable bandwidth, and ii) the shape of the transmitted pulses is not important, since the total energy received is not shape dependent.

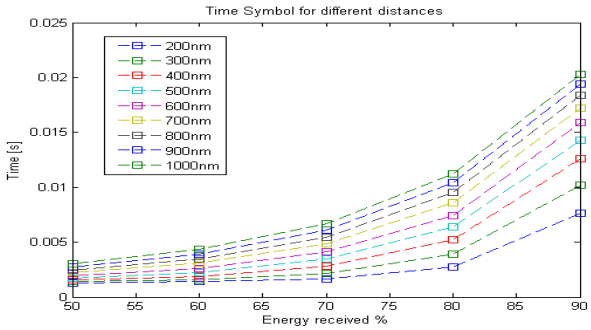

Fig. 8. Symbol duration according to the percentage of received energy for several distances. The transmission distance ranges from 200 nm to 1000 nm.

VII. Evaluation of Pulse-based Modulation Techniques

Communication of larger amounts of information can be achieved by transmitting a train of pulses, and by changing one or more of their parameters. In this section, we evaluate two basic modulation techniques for trains of pulses, namely, the Pulse Amplitude Modulation (PAM), and the Pulse Position Modulation (PPM), which are well-suited to this communication technique, where nanomachines are expected to be very simple devices. We use Gaussian pulse shapes for this analysis.

Any transmitted signal suffers a time widening dependent on the distance between the transmitter and the receiver. In order to avoid Inter-Symbol Interference (ISI), which can create undecodable sequences at the receiver side, a guard time between symbols is added in transmission. The *symbol time*, T_s, is the sum of the symbol duration and the guard time.

In this analysis, we use two different symbol times, corresponding to the time instant when the 90% and the 50% of the total symbol energy is received, which correspond to $T_s = 0.02s$ and $T_s = 0.003$, respectively, for a transmission distance of 1000 nm. Fig. 8 shows how the symbol time increases with the distance.

We consider a particular case of the binary PAM modulation known as On-Off Keying (OOK). In this modulation, a logical "1" is transmitted by sending a Gaussian pulse at the beginning of the *symbol time*, and a logical "0" is transmitted as silence. This scheme is compared with a binary PPM modulation, which requires to divide the *symbol time* in two halves, and codifies a logical "1" by transmitting a pulse during the first half of the *symbol time*, and a logical "0" by transmitting a pulse during the second half.

To evaluate both techniques under the same conditions, the same energy per symbol is transmitted in each of them. This means that, in PPM, the energy of each pulse is half of that in PAM. For this reason, we expect a larger transmission range using PAM. The ISI of the PPM modulation in the case of transmitting a logical "0" followed by a "1" is also expected to be higher.

Fig. 9 shows the a comparison of the performance of OOK and PPM. The transmitted sequence is "0110110001". The upper image shows the received signal when the *symbol time*

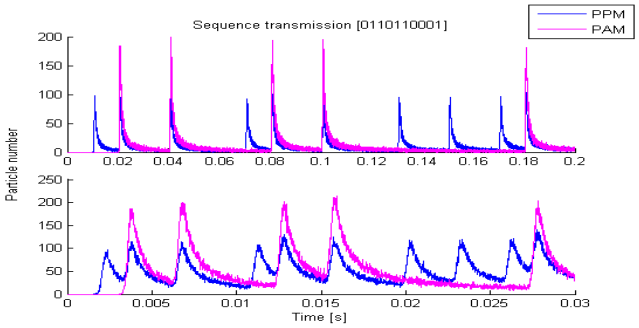

Fig. 9. Comparison of the OOK and PPM modulations for a transmission distance of 1000 nm

corresponds to 90% of the pulse energy. OOK pulses are received with more energy, thus allowing to cover a larger range in a broadcast communication. The lower image shows the result of the transmission for a shorter *symbol time*, with similar results. Overall, PPM yields to a higher ISI, as expected.

To summarize, OOK outperforms PPM since the average number of transmitted pulses with OOK is half of the number of pulses required for PPM. As a consequence, the transmitter can encode the OOK pulses using twice as much energy as with PPM. OOK pulses reach the receiver with a higher power compared to PPM pulses and they are easier to decode. Since in OOK one of the symbols is transmitted as a silence, the ISI is reduced. We conclude that OOK is the most convenient modulation scheme for the molecular diffusion-based channel.

VIII. Conclusion

In this work, we detail different diffusion-based scenarios that can be simulated through *NanoSim* according different assumptions on the physical layer. We have proved the linearity and temporal invariance of the diffusion-based molecular communication channel in the case of free diffusion, by simulating the motion of each particle with Brownian dynamics as well as by including elastic collisions as interactions. We have validated the diffusion-noise when the receiver estimates the concentration by counting the number of molecules in its sensing area, with the Particle Counting Noise model from [22].

After a pulse shaping analysis, we conclude that, the transmission of the shortest possible pulses is needed to reach a given distance range while having the maximum possible bandwidth available. Ideally, the optimal pulse shape is a spike of particles with zero length. The total transmitted energy for a symbol determines its transmission range, and this does not depend on the shape of the pulse. After the comparison of two basic pulse-based communication schemes, we conclude that OOK is the most efficient binary modulation scheme for the diffusion-based molecular communication channel.

We believe that the future work on this topic can take advantage from the results presented in this paper. In particular, these results point out that in an molecular nanonetwork, in oder to minimize the overall energy consumption while allowing for a correct reception of the transmitted signal, the transmitter nanomachines should be able to adjust the energy and the duration of the transmitter pulses. While this can be in contrast with the basic capabilities expected by the nanomachines, we believe that a series of suboptimal schemes can be studied in order to meet possible performance limitations.

References

[1] I. F. Akyildiz, F. Brunetti, and C. Blàzquez, "Nanonetworks: A new communication paradigm," *Computer Networks*, vol. 52, pp. 2260 – 2279, 2008.

[2] M. Moore, A. Enomoto, T. Nakano, R. Egashira, T. Suda, A. Kayasuga, H. Kojima, H. Sakakibara, and K. Oiwa, "A Design of a Molecular Communication System for Nanomachines Using Molecular Motors," *IEEE International Conference on Pervasive Computing and Communications*, 2006.

[3] L. J. Q. N. T. Liu, J. Q. and T. Nakano, "An information theoretic model of molecular communication based on cellular signaling," *1st International ICST Workshop on Computing and Communications from Biological Systems: Theory and Applications*, May 2007.

[4] T. Nakano, T. Suda, M. Moore, R. Egashira, A. Enomoto, and K. Arima, "Molecular communication for nanomachines using intercellular calcium signaling," *Fifth IEEE Conference on Nanotechnology*, vol. 2, pp. 478–481.

[5] M. Gregori and I. F. Akyildiz, "A new nanonetwork architecture using flagellated bacteria and catalytic nanomotors," *IEEE J.Sel. A. Commun.*, vol. 28, no. 4, pp. 612–619, 2010.

[6] I. F. Akyildiz and P. Lluis, "Molecular Communication Options for Long Range Nanonetworks," *Computer Networks*, vol. 53, no. 16, pp. 2753–2766, 2009.

[7] M. Pierobon and I. F. Akyildiz, "A physical End to End Model for Molecular Communication in Nanonetworks," *Journal of Selected Areas in Communications (JSAC)*, 2010.

[8] G. A. Silva, "Introduction to nanotechnology and its applications to medicine," *Surgical Neurology*, vol. 61, pp. 216 – 220, 2004.

[9] R. A. Freitas, "Nanotechnology, nanomedicine and nanosurgery." *International Journal of Surgery*, vol. 3, no. 4, pp. 243–6, Jan. 2005. [Online]. Available: http://www.ncbi.nlm.nih.gov/pubmed/17462292

[10] I. Malsch, "Biomedical applications of nanotechnology," *The Industrial Physicist*.

[11] M. Pierobon and I. F. Akyildiz, "Information capacity of diffusion-based molecular communication in nanonetworks," *Proc. IEEE Infocom Miniconference*, 2011.

[12] B. Atakan and B. O. Akan, "Deterministic capacity of information flow in molecular nanonetworks," *NanoCommunication Networks*, 2010.

[13] B. Atakan and O. B. Akan, "On Channel Capacity and Error Compensation in Molecular Communication," *Springer Transactions on Computational Systems Biology*, vol. 10, pp. 59–80, 2008.

[14] R. Kadloor, S. Adve, "A framework to study the molecular communication system," *Computer Communications and Networks, 2009. ICCCN 2009. Proceedings of 18th Internatonal Conference on*, 2009.

[15] E. Gul and O. B. Akan, "NanoNS: A Nanoscale Network Simulator Framework for Molecular Communications," *To appear in Nano Communication Networks (Elsevier)*, 2010.

[16] M. J. Moore. [Online]. Available: http://www.ics.uci.edu/~mikemo/

[17] J. Philibert, "One and a half century of diffusion: Fick, einstein, before and beyond," *Diffusion Fundamentals*, pp. 1.1–1.10, 2005.

[18] T. S. Ursell, "The Diffusion Equation A Multi-dimensional Tutorial," Pasadena, 2007. [Online]. Available: http://www.rpgroup.caltech.edu/~natsirt/aph162/diffusion.pdf

[19] D. L. Ermak and J. A. Mccammon, "Brownian dynamics with hydrodynamic interactions," *J. Chem. Phys.*, vol. 69, pp. 1352–1360, 1978.

[20] L. Vlahos, H. Isliker, Y. Kominis, and K. Hizanidis. (2008, May) Normal and Anomalous Diffusion: A Tutorial. [Online]. Available: http://arxiv.org/abs/0805.0419

[21] F. S. H. W. Mndez, V, *Reaction-Transport Systems: Mesoscopic Foundations, Fronts, and Spatial Instabilities*. Springer, 2010.

[22] M. Pierobon and I. F. Akyildiz, "Diffusion-based Noise Analysis for Molecular Communication in Nanonetworks," *to appear in IEEE Transactions on Signal Processing, 2011.*